



"The human primary somatosensory cortex is differentially involved in vibrotaction and nociception."

Lenoir, Cédric ; Huang, Gan ; Vandermeeren, Yves ; Hatem, Samar ; Mouraux, André

Abstract

The role of the primary somatosensory cortex (S1) in vibrotaction is well established. In contrast, its involvement in nociception remains debated. Here, we test whether S1 is similarly involved in the processing of non-nociceptive and nociceptive somatosensory input in humans by comparing the after-effects of high-definition transcranial direct current stimulation (HD-tDCS) of the primary sensorimotor cortex on the event-related potentials (ERPs) elicited by non-nociceptive and nociceptive somatosensory stimuli delivered to the ipsilateral and contralateral hand. Cathodal HD-tDCS significantly affected the responses to non-nociceptive somatosensory stimuli delivered to the contralateral hand: both early-latency ERPs from within S1 (N20 wave elicited by transcutaneous electrical stimulation of the median nerve) and late-latency ERPs elicited outside S1 (N120 wave elicited by short-lasting mechanical vibrations delivered to the index fingertip, thought to originate from bilateral oper...

Document type : *Article de périodique (Journal article)*

Référence bibliographique

Lenoir, Cédric ; Huang, Gan ; Vandermeeren, Yves ; Hatem, Samar ; Mouraux, André. *The human primary somatosensory cortex is differentially involved in vibrotaction and nociception..* In: *Journal of Neurophysiology*, (26 avril 2017)

1 **The human primary somatosensory cortex is differentially involved in vibrotaction and**
2 **nociception**

3
4 Author names and affiliations

5 Cédric Lenoir¹, Gan Huang¹, Yves. Vandermeeren^{1,2,3}, Samar Marie Hatem^{1,4}, André
6 Mouraux¹

7
8 abbreviated title

9 **S1 is differently involved in vibrotaction and nociception**

10
11
12 ¹ Université catholique de Louvain (UCL), Institute of Neuroscience (IONS) avenue Mounier
13 53, 1200 Brussels Belgium
14 cedric.lenoir@uclouvain.be (orcid.org/0000-0002-1420-7550)
15 gan.huang@uclouvain.be
16 andre.mouraux@uclouvain.be
17

18
19 ² UCL, CHU UCL Namur (Godinne), Neurology Department, NeuroModulation Unit (NeMU),
20 rue Dr Therasse 1, 5530 Yvoir, Belgium
21

22
23 ³ UCL, Louvain Bionics, UCL, Louvain-la-Neuve, Belgium
24 yves.vandermeeren@uclouvain.be
25

26
27 ⁴ Physical Medicine and Rehabilitation, Brugmann University Hospital Place Van Gehuchten
28 4, 1020 Brussels Belgium, Vrije Universiteit Brussel, Université Libre de Bruxelles, Brussels,
29 Belgium
30 samar.hatem@chu-brugmann.be
31

32
33
34 Corresponding author:
35 André Mouraux
36 Institute of Neuroscience (IoNS)
37 53, Avenue Mounier (B1.53.02)
38 Université catholique de Louvain
39 B-1200 Brussels
40 Belgium
41 E-mail: andre.mouraux@uclouvain.be
42 Telephone: +32(0)2 764 54 47

43 **Abstract**

44 The role of the primary somatosensory cortex (S1) in vibrotaction is well established. In
45 contrast, its involvement in nociception remains debated. Here, we test whether S1 is
46 similarly involved in the processing of non-nociceptive and nociceptive somatosensory input
47 in humans by comparing the after-effects of high-definition transcranial direct current
48 stimulation (HD-tDCS) of the primary sensorimotor cortex on the event-related potentials
49 (ERPs) elicited by non-nociceptive and nociceptive somatosensory stimuli delivered to the
50 ipsilateral and contralateral hand. Cathodal HD-tDCS significantly affected the responses to
51 non-nociceptive somatosensory stimuli delivered to the contralateral hand: both early-
52 latency ERPs from within S1 (N20 wave elicited by transcutaneous electrical stimulation of
53 the median nerve) and late-latency ERPs elicited outside S1 (N120 wave elicited by short-
54 lasting mechanical vibrations delivered to the index fingertip, thought to originate from
55 bilateral operculo-insular and cingulate cortices). These results support the notion that S1
56 constitutes an obligatory relay for the cortical processing of non-nociceptive tactile input
57 originating from the contralateral hemibody. Contrasting with this asymmetric effect of HD-
58 tDCS on the responses to non-nociceptive somatosensory input, HD-tDCS over the
59 sensorimotor cortex led to a bilateral and symmetric reduction of the magnitude of the
60 N240 wave of nociceptive laser-evoked potentials elicited by stimulation of the hand
61 dorsum. Taken together, our results demonstrate, in humans, a differential involvement of
62 S1 in vibrotaction and nociception.

63

64

65 **Keywords**

66 evoked potentials, nociception, touch, primary somatosensory cortex, transcranial direct
67 current stimulation

68

69 **New & Noteworthy**

70 Whereas the role of the primary somatosensory cortex (S1) in vibrotaction is well
71 established, its involvement in nociception remains strongly debated. By assessing, in
72 healthy volunteers, the effect of high-definition transcranial direct current stimulation (HD-
73 tDCS) over S1, we demonstrate a differential involvement of S1 in vibrotaction and
74 nociception.

75 1. INTRODUCTION

76 The role of the primary somatosensory cortex (S1) in vibrotaction is well established
77 (Abraira and Ginty 2013). In contrast, its involvement in nociception remains elusive
78 (Bushnell et al. 1999). For example, lesions of S1 markedly impair many aspects of tactile
79 perception (Penfield and Boldrey 1937), but have little or no long-standing effect on the
80 ability to perceive pain (Head and Holmes 1911). Similarly, focal seizures of S1 and direct
81 electrical stimulation of S1 in awake patients undergoing surgery for epilepsy can generate
82 vivid touch-related paresthesiaes, but do not appear to elicit pain (Mazzola et al. 2012;
83 Penfield 1947; Tuxhorn 2005). Also supporting the notion that S1 is involved differentially in
84 the processing of touch and pain is the observation, in animals, that S1 is not the main
85 projection site of nociceptive spinothalamic input which, instead, projects predominantly to
86 the insula, the secondary somatosensory cortex (S2) and the cingulate cortex (Dum et al.
87 2009). Nevertheless, functional neuroimaging studies using magnetic resonance imaging
88 (MRI) or positron emission tomography (PET) have shown that nociceptive stimuli elicit a
89 clear haemodynamic response in the contralateral S1, at a location corresponding to the
90 somatotopic representation of the stimulated body site (Bushnell et al. 1999; Chen et al.
91 2011; Chen et al. 2012; Coghill et al. 1994; Hu et al. 2015). Electrophysiological studies using
92 electroencephalography (EEG), magnetoencephalography (MEG) and intracerebral
93 recordings have provided less consistent findings, but still suggest that nociceptive stimuli
94 elicit responses in the contralateral S1, at latencies compatible with the earliest stages of
95 the cortical processing of nociceptive inputs (Kanda et al. 2000; Ploner et al. 1999; Ploner et
96 al. 2002; Tarkka and Treede 1993; Valentini et al. 2012).

97 Finally, studies have attempted to assess the differential involvement of S1 in touch and
98 pain by characterizing the effect of repetitive transcranial magnetic stimulation (rTMS) over
99 S1 on the perception and event-related brain potentials (ERPs) elicited by non-nociceptive
100 and nociceptive somatosensory stimuli delivered to the ipsilateral and contralateral
101 hemibody (Poreisz et al. 2008a; Torta et al. 2013). This approach is highly relevant because,
102 unlike studies based on sluggish haemodynamic responses sampled using functional
103 neuroimaging techniques, studies based on the direct sampling of cortical activity using
104 ERPs have the temporal resolution required to tease out S1 responses related to the early
105 stages of the cortical processing of ascending somatosensory input from late responses
106 triggered by re-entrant feedback projections to S1 originating from higher-order cortical
107 areas. Unfortunately, the results of these studies were largely inconclusive, mainly because
108 they failed to demonstrate any clear and reproducible effect of rTMS on the excitability of
109 S1. For instance, using various protocols of theta-burst stimulation (TBS, a special form of
110 rTMS), Poreisz et al. (2008a) showed that rTMS delivered over S1 reduces the magnitude of
111 the N240 wave of nociceptive laser-evoked brain potentials elicited by stimulation of the
112 contralateral hand, but they did not compare directly this effect to the effect on the
113 responses elicited by stimulation of the ipsilateral hand. Such a direct comparison was
114 performed by Torta et al. (2013). In that study, they assessed the effects of TBS delivered
115 over the primary motor cortex (M1) and S1 on the ERPs elicited by both non-nociceptive
116 and nociceptive stimuli delivered to the two hands, but failed to disclose any specific effect
117 of TBS on the responses elicited by stimulation of the contralateral hand. These inconstant
118 findings could be related to the increasingly acknowledged large interindividual variability of
119 the effects of rTMS delivered over the sensorimotor cortex. For example, Hamada et al.
120 (2013) and Huang and Mouraux (2015) recently showed that continuous TBS delivered over

121 M1 decreases motor excitability in some individuals, whereas it increases motor excitability
122 in a similar number of other individuals.

123 Here, in a first experiment we attempt to determine whether S1 is involved differentially in
124 the processing of touch and pain using another non-invasive technique to modulate the
125 excitability of the human sensorimotor cortex: cathodal high-definition transcranial direct
126 current stimulation (HD-tDCS). The frequently proposed mechanism of cathodal tDCS is that
127 neuronal populations located below the cathode become hyperpolarized, thereby reducing
128 their excitability (Datta et al. 2009; Nitsche et al. 2008; Nitsche and Paulus 2000). The
129 cathode electrode was placed over the expected hand representation of the left or right S1,
130 surrounded by four return anode electrodes placed on a 5-cm radius circle. Previous studies
131 have shown that the neuromodulation induced by this 4x1 ring HD-tDCS montage is much
132 more focal than the neuromodulation induced by the conventional tDCS configuration
133 consisting of two large rectangular electrodes (Datta et al. 2009; Edwards et al. 2013; Kuo et
134 al. 2013; Villamar et al. 2013), and comparable to that of TMS delivered using a 75 mm
135 figure-of-eight coil (Edwards et al. 2013). This allowed us to compare, within-subjects, the
136 after-effects of HD-tDCS applied for 20 minutes over S1 on the perception and ERPs elicited
137 by non-nociceptive and nociceptive stimuli delivered to the ipsilateral and contralateral
138 hand relative to the hemisphere onto which HD-tDCS was applied.

139 Transcutaneous electrical stimulation of the median nerve at the level of the wrist was used
140 to compare the effects of HD-tDCS on the early-latency response of S1 to non-nociceptive
141 somatosensory input originating from the contralateral and ipsilateral hands and, thereby,
142 to confirm the specific neuromodulatory effect of HD-tDCS on S1. Within the same
143 experimental sessions, mechanical vibrotactile stimuli and thermal nociceptive stimuli were

144 delivered to the left and right hands to assess whether modulating the state of the
145 sensorimotor cortex exerts a differential effect on the cortical processing of non-nociceptive
146 and nociceptive somatosensory inputs. We hypothesized that, if S1 constitutes an obligatory
147 relay for the cortical processing of somatic input originating from the contralateral
148 hemibody, HD-tDCS delivered over the hand representation of the sensorimotor cortex
149 would affect differently the ERPs elicited by stimulation of the contralateral hand vs. the
150 ipsilateral hand.

151 Finally, we conducted a second experiment in another group of participants. This
152 experiment was identical to the first experiment except for the fact that cathodal HD-tDCS
153 was applied for only 30 seconds. Comparison of the after-effects of real HD-tDCS (HD-tDCS
154 experiment) and sham HD-tDCS (sham experiment) allowed us to test whether the effect on
155 the processing of non-nociceptive and nociceptive somatosensory input were due to a true
156 neuromodulatory effect of 20 minutes of HD-tDCS or to unrelated time-dependent effects.

157 **2. MATERIALS AND METHODS**

158 **2.1. Participants**

159 Fourteen healthy right-handed volunteers were included in a first experiment assessing the
160 effect of cathodal HD-tDCS over the sensorimotor cortex on the perception and ERPs
161 elicited by non-nociceptive and nociceptive stimuli delivered to the ipsilateral and
162 contralateral hand relative to the hemisphere onto which HD-tDCS was applied (*HD-tDCS*
163 *experiment*: 12 women/2 men; 23.2 ± 1.1 years; *mean \pm SD*; range 21-25). Fourteen other
164 participants took part in a second experiment in which real HD-tDCS (20 minutes of
165 stimulation) was replaced by sham HD-tDCS (30 s of stimulation) (*sham experiment*: 8
166 women/6 men; 27.3 ± 4.7 years; range 22-35). All participants were blinded to the aims of

167 the study. Because participants took part in one or the other experiment, all subjects were
168 equally naïve with the procedures when coming to their first and only session. Handedness
169 was assessed using The Flinders Handedness survey (FLANDERS) (Nicholls et al. 2013).
170 Because the skin reflectance, absorption and transmittance of the infrared radiations
171 generated by the Neodymium:Yttrium-Aluminum-Perovskite (Nd:YAP) laser used to deliver
172 nociceptive stimuli (wavelength: 1.34 μm) are highly dependent on skin pigmentation, only
173 participants with light skin were recruited. They were recruited among students and staff of
174 the university. All participants were screened by a neurologist for contra-indications to tDCS
175 (Nitsche et al. 2008). None of them had any history of psychiatric or neurological disorders
176 including epilepsy or family history of seizure. The experimental procedures were approved
177 by the Ethics Committee (*Commission d'Éthique Biomédicale Hospitalo-Facultaire*) of the
178 Université catholique de Louvain (UCL) (B403201316436) and all participants provided a
179 written informed consent.

180 **2.2. Experimental design**

181 *HD-tDCS experiment.* Subjects were comfortably seated on a reclining chair during the entire
182 experiment, consisting of two successive EEG recording sessions, immediately before and
183 immediately after applying cathodal HD-tDCS over the left or right sensorimotor cortex (Fig.
184 1). The side of stimulation was counterbalanced across participants. The second recording
185 always began within 5 minutes and ended within 25 minutes of the end of HD-tDCS. Each
186 EEG recording consisted of four blocks whose order was counterbalanced across subjects. In
187 two separate blocks, transcutaneous electrical nerve stimuli were delivered to the left or
188 right median nerve to characterize the early-latency N20 wave, i.e. the first cortical
189 response to non-nociceptive somatosensory input ascending through lemniscal pathways. A

190 total of 500 stimuli were delivered to each hand, using a constant 0.25 s inter-stimulus
191 interval (ISI). In a third block, non-nociceptive vibrotactile stimuli were applied to the left
192 and right index fingertip to elicit ERPs related to the selective activation of tactile
193 mechanoreceptors. In a fourth block, nociceptive laser stimuli were applied to the left and
194 right hand dorsum to elicit ERPs related to the selective activation of heat-sensitive A δ -fiber
195 nociceptors. In these blocks, the stimuli were delivered randomly to the left or right hand
196 using a random 5-7 s ISI. A total of 25 stimuli were delivered to each hand. After each
197 stimulus, participants were asked to verbally report the intensity of perception using a
198 numerical rating scale (NRS) ranging from 0 (no sensation) to 10 (most intense sensation), 5
199 marking the border between non-painful and painful domains of sensation.

200 *Sham experiment.* The sham experiment was identical to the HD-tDCS experiment except for
201 the fact that participants received sham cathodal HD-tDCS instead of real HD-tDCS over the
202 left or right sensorimotor cortex. Such as in the HD-tDCS experiment, the stimulation
203 procedure lasted 20 minutes. However, the duration of actual current stimulation lasted less
204 than two minutes (Fig. 1).

205 **2.3. Cathodal HD-tDCS**

206 Cathodal HD-tDCS was delivered for 20 minutes using a 4x1 ring montage of five Ag-AgCl
207 sintered ring electrodes (B10 EasyCap GmbH, Germany), inserted in a ring electrode adapter
208 to increase the area of contact between the electrode, gel and skin (electrode-gel contact
209 area: 100 mm²; gel-skin contact area : > 1.5 cm²) (Minhas et al. 2010). The 4x1 ring montage
210 consisted of one cathode electrode placed over the International 10-20 position C3 or C4,
211 surrounded by four return anode electrodes placed on a circle of approximately 5 cm radius
212 around the cathode (FC5, FC1, CP1, CP5 or FC6, FC2, CP2, CP6). Edwards et al. demonstrated

213 using electric field modeling and by comparing the effects on motor excitability of HD-tDCS
214 delivered at adjacent positions relative to M1, that the focal aspect of HD-tDCS delivered
215 using this 4x1 montage is comparable to that of TMS delivered using a 75 mm figure-of-
216 eight coil (Edwards et al. 2013). Impedances between the cathode electrode and each
217 anode electrode were kept below 5 k Ω . The stimulation was generated using a constant
218 current electrical stimulator (Eldith, NeuroConn GmbH, Germany). In the HD-tDCS
219 experiment, the current was ramped up from 0 to 1 mA during the first 40 s of stimulation,
220 and was then maintained constant during 20 minutes. At the end of these 20 minutes, the
221 current was ramped down in 40 s. In the sham experiment, the stimulation protocol also
222 lasted 20 minutes. However, the actual duration of the stimulation was set to 30 s. Such as
223 in previous studies (Borckardt et al. 2012; Minhas et al. 2010), both real HD-tDCS and sham
224 HD-tDCS elicited a moderate tingling and itching sensation at the site of stimulation.
225 Because this sensation faded within a couple of minutes even when HD-tDCS was
226 maintained for 20 minutes, the sensations generated by real HD-tDCS and sham HD-tDCS
227 were highly similar and, most probably, indistinguishable.

228 **2.4. Non-nociceptive and nociceptive somatosensory stimuli**

229 *Non-nociceptive transcutaneous electrical stimulation of the median nerve* was used to
230 assess in a reliable fashion the early-latency S1 response elicited by non-nociceptive
231 somatosensory input ascending through the lemniscal pathway (i.e., the N20 wave). The
232 stimuli consisted of non-painful constant-current square-wave (0.5 ms) electrical pulses
233 generated using a DS7 stimulator (Digitimer Ltd, Letchworth, UK) and delivered using a pair
234 of 24 mm diameter adhesive electrodes (Covidien Kendall Disposable Surface
235 EMG/ECG/EKG, Mansfield, USA) separated by a 2 cm inter-electrode distance, placed over

236 the median nerve at the level of the wrist. The cathode electrode was positioned proximal
237 relative to the anode electrode. The intensity of stimulation (7.1 ± 1.8 mA) was set such as
238 to elicit a consistent and visible twitch of the thumb. The same intensity of stimulation was
239 used before and after HD-tDCS, and the adhesive electrodes were not displaced.

240 *Non-nociceptive vibrotactile stimuli* were short-lasting (50 ms) mechanical vibrations (300
241 Hz) delivered on the index fingertip using a vibrotactile transducer (length: 2.8 cm; width:
242 1.2 cm; Haptuators; Tactile Labs, Montreal, Canada). The index fingertip was chosen
243 because of the important density of Pacinian mechanoreceptors in that skin area (Abraira
244 and Ginty 2013). During vibrotactile stimulation, white noise was played through
245 headphones to avoid any auditory response to the sound produced by the transducers.

246 *Nociceptive heat stimuli* were short-lasting (5 ms) pulses of radiant heat delivered on the
247 hand dorsum using an Nd:YAP laser (wavelength, $1.34 \mu\text{m}$; EEn Group, Firenze, Italy). The
248 hand dorsum was chosen to avoid issues related to the conduction of heat within the
249 thicker skin of the fingertip. Beam diameter at target site was set to 5 mm. The energy of
250 the stimulus (2.0 ± 0.2 J) was adjusted individually such as to elicit a clear pinprick sensation
251 detected with a reaction time shorter than 650 ms, i.e. a reaction time compatible with the
252 conduction velocity of A δ fibers (Mouraux et al. 2003; Plaghki et al. 1994; Towell et al.
253 1996). The same energy was used before and after HD-tDCS. The target of the laser stimulus
254 was slightly displaced after each trial such as to avoid nociceptor habituation and/or
255 sensitization.

256 **2.5. EEG recording**

257 The EEG was recorded at a sampling rate of 4000 Hz using an average reference (32-channel
258 ASA-LAB EEG system; Advanced Neuro Technologies, The Netherlands), with 32 actively

259 shielded Ag-AgCl electrodes mounted in an elastic electrode cap and arranged according to
260 the International 10-20 system (EasyCap 32, EASYCAP GmbH, Germany). During the entire
261 EEG recording, participants were instructed to keep their gaze fixed on a black cross
262 displayed in front of them and to sit as still as possible. Eye movements were recorded using
263 two adhesive surface electrodes placed at the upper-right and lower-left sides of the left
264 eye. Impedances were kept below 5 k Ω for all leads. The continuous EEG recordings were
265 processed offline using Letswave6 (<http://www.nocions.org/letswave6>).

266 **2.6. ERP waveforms**

267 *Non-nociceptive ERPs elicited by transcutaneous electrical stimulation of the median nerve.*

268 Within the continuous EEG recordings, the electrical stimulation artefact was suppressed
269 using a linear interpolation of the signals recorded from -1 to +7 ms relative to stimulation
270 onset. The recordings were then high-pass filtered using a 0.3 Hz Butterworth zero phase
271 filter and segmented into 0.2 s epochs ranging from -0.05 to +0.15 s. Artefacts due to eye
272 blinks or eye movements were removed using a validated method based on an
273 independent-component analysis (FastICA algorithm) (Hyvarinen and Oja 2000). After
274 applying a baseline correction (subtraction of the average amplitude of the signal within the
275 reference interval 7-11 ms), the signals were re-referenced to Fz. Epochs containing signals
276 exceeding ± 75 μ V were rejected to reduce the contribution of artefacts such as head
277 movements, eye blinks or muscular activity. Finally, average waveforms were computed for
278 each participant, session and stimulation side. Within these waveforms, the N20 wave was
279 identified as the most negative deflection occurring 17-23 ms after stimulus presentation
280 (Fig. 2), at the parietal electrode contralateral to the stimulated hand (left hand : P4; right
281 hand : P3) (Cruccu et al. 2008).

282 *Non-nociceptive vibrotactile ERPs and nociceptive laser ERPs.* After applying a 0.3-40 Hz
283 Butterworth zero phase band pass filter, the continuous recordings were segmented into 3 s
284 epochs ranging from -0.5 to +2.5 s relative to stimulus onset. Artefacts due to eye blinks or
285 eye movements were removed using the FastICA algorithm (Hyvarinen and Oja 2000). After
286 baseline correction (reference interval -0.5 to 0 s), epochs containing signals exceeding ± 75
287 μV were rejected before computing separate average waveforms for each participant,
288 session, stimulation type and stimulation side. Within the non-nociceptive vibrotactile ERP
289 waveforms, two distinct peaks (N120 and P250) were identified at electrode Cz, referenced
290 to M1M2 (Garcia-Larrea et al. 1995; Kenntner-Mabiala et al. 2008; Miltner et al. 1989). The
291 N120 was defined as the most negative deflection peaking 90-160 ms after stimulus onset.
292 The P250 was defined as the most positive deflection following the N120 (Fig. 2). Within the
293 nociceptive laser ERP waveforms, three distinct peaks were identified (N160, N240 and
294 P350) (Bromm and Treede 1984; Cruccu et al. 2008; Hu et al. 2010; Treede et al. 1988). At
295 electrode Cz referenced to M1M2, the N240 was identified as the most negative deflection
296 peaking 140-260 ms after stimulus presentation, and the P350 as the most positive
297 deflection following the N240 (Fig. 2). The N160 was defined as the most negative deflection
298 peaking 140-220 ms at the central electrode C3 or C4 contralateral electrode to the
299 stimulated hand, and referenced to Fz (Bromm and Treede 1984; Treede et al. 1988).

300 **2.7. High-frequency oscillations (HFOs)**

301 Previous studies have shown that, in addition to the N20 waveform, transcutaneous
302 electrical stimulation of the median nerve also elicits an early-latency burst of high-
303 frequency oscillations (HFOs: 400-900 Hz) (Ozaki and Hashimoto 2011). These HFOs are
304 commonly separated in an early component thought to be generated by thalamocortical

305 and pyramidal neurons, and a late component reflecting inhibitory interneuronal S1 activity
306 (Ozaki and Hashimoto 2011; Restuccia et al. 2011). Such HFOs have not been reported using
307 mechanical stimulation of skin receptors, probably because identifying this high frequency
308 activity requires a very phasic stimulus repeated a large number of times (Katayama et al.
309 2010).

310 To evaluate the effects of HD-tDCS on the magnitude of the HFOs elicited by stimulation of
311 the ipsilateral and contralateral median nerve, the continuous EEG recordings were band-
312 pass filtered using a 400-1000 Hz bandpass Butterworth zero phase filter after suppression
313 of the electrical stimulation artefact (-1 to 7 ms), and segmented into 0.2 s epochs ranging
314 from -0.05 to +0.15 s relative to stimulus onset. A baseline correction (reference interval 7
315 to 11 ms) was performed and the signals were averaged across trials after re-referencing to
316 Fz. A Hilbert transform was then used to obtain an estimate of the envelope of HFOs
317 (Restuccia et al. 2011). Such as in previous studies (Katayama et al. 2010; Restuccia et al.
318 2007), the early and late subcomponents of HFOs were defined relative to the latency of the
319 N20 wave. The early subcomponent extended between -5 and 0 ms relative to the N20
320 peak, and the late subcomponent extended between 0 and +8 ms (Fig. 3A). The magnitudes
321 of these two subcomponents were estimated by averaging the result of the Hilbert
322 transform within these two intervals. Averaged across participants and conditions, the
323 amplitude of HFOs were maximal at the central-parietal electrodes contralateral to the
324 stimulated hand (left hand : CP6; right hand : CP5) (Fig. 3B). These electrodes were thus
325 chosen to estimate the magnitude of early and late HFOs across participants and conditions.

326 **2.8. Statistical analyses**

327 A mixed-model ANOVA with the between-subject factor 'group' (real HD-tDCS vs. sham HD-
328 tDCS) and the within-subject factors 'time' (before vs. after HD-tDCS) and 'side'
329 (somatosensory stimuli delivered to the ipsilateral vs. contralateral hand relative to the
330 sensorimotor cortex onto which the neuromodulation was applied) was used to test directly
331 the differential effects of real vs. sham HD-tDCS on the perception and ERPs elicited by
332 nociceptive and non-nociceptive stimuli delivered to the ipsilateral and contralateral hands.
333 Indeed, a significant three-way interaction between the factors 'group', 'time' and 'side'
334 would demonstrate a differential effect of HD-tDCS vs. sham stimulation on the responses
335 to stimuli delivered to the ipsilateral vs. contralateral hand; whereas a two-way 'time' x
336 'group' interaction would indicate a bilateral effect of HD-tDCS vs. sham stimulation, and a
337 two-way 'time' x 'side' interaction would indicate an asymmetric effect on the responses to
338 stimuli delivered to the ipsilateral vs. contralateral hands present both after real and sham
339 HD-tDCS. Finally, a main effect of 'time' would indicate a bilateral change in the responses.

340 In a second step, the effects of real HD-tDCS and sham HD-tDCS were assessed within each
341 experiment separately using a repeated-measures ANOVAs with the within-subject factors
342 'time' (before vs. after HD-tDCS) and 'side' (somatosensory stimuli delivered to the
343 ipsilateral vs. contralateral hand relative to the hemisphere onto which the
344 neuromodulation was applied).

345 A Greenhouse-Geisser correction was used when necessary. When a significant interaction
346 was found, post-hoc pairwise comparison or paired t-tests were performed. Significance
347 threshold was set at $p < .05$.

348 **3. RESULTS**

349 **3.1. Intensity of perception**

350 The intensity of the percept elicited by non-nociceptive tactile stimuli were largely
351 unchanged (Figure 4). Accordingly, the mixed-model ANOVA showed no main effect of
352 'time' ($F(1,26) = .013$; $p = .908$), and no interaction between the factor 'time' and the factors
353 'group' or 'side' (Table 1).

354 In contrast, the intensity of the percept elicited by nociceptive laser stimuli was reduced
355 both after real HD-tDCS and after sham HD-tDCS. This reduction was symmetric at both
356 hands and, on average, more pronounced in the group that received real HD-tDCS (average
357 reduction at both hands: -15 to -20%) as compared to the group that received sham HD-
358 tDCS (average reduction at both hands: -1 to -11%). The mixed-model ANOVA confirmed a
359 main effect of 'time' ($F(1,26) = 11.4$; $p = .002$), but showed no significant interaction
360 between the factor 'time' and the factors 'group' or 'side' (Table 1). The within-subject
361 ANOVAs conducted separately for each experiment showed a significant main effect of
362 'time' in the HD-tDCS experiment ($F(1,13) = 9.4$; $p = .009$), but not in the sham experiment
363 ($F(1,13) = 2.57$; $p = .133$) (Tables 2 and 3, Figure 4).

364 **3.2. Early-latency ERPs elicited by electrical stimulation of the median nerve**

365 Transcutaneous electrical stimulation of the median nerve elicited a consistent N20 wave in
366 each participant and condition (Fig. 2). As compared to the N20 wave elicited by stimulation
367 of the hand ipsilateral to the sensorimotor cortex onto which HD-tDCS was applied, the
368 magnitude of the N20 wave elicited by stimulation of the contralateral hand was, on
369 average, reduced both after real HD-tDCS and after sham HD-tDCS. This asymmetric
370 reduction in amplitude was more pronounced after real HD-tDCS as compared to sham HD-
371 tDCS. This observation was confirmed by the mixed-model ANOVA, which showed a
372 significant interaction between the factors 'time' and 'side' ($F(1,26) = 8.42$; $p = .007$), but no

373 significant interaction between these two factors and the between-subject factor 'group'
374 ($F(1,26) = 2.07$; $p = .163$; Table 1). In the HD-tDCS experiment, the within-subject ANOVA
375 showed a significant 'time' x 'side' interaction ($F(1,13)=9.27$; $p=.009$; Table 2), and post-hoc
376 comparisons confirmed that, after real HD-tDCS, the magnitude of the N20 wave elicited by
377 stimulation of the contralateral hand was significantly reduced ($-0.31 \pm 0.48 \mu\text{V}$; $t = 2.436$; $p =$
378 $.030$), whereas the magnitude of the N20 wave elicited by stimulation of the ipsilateral
379 hand tended to increase ($+0.28 \pm 0.69 \mu\text{V}$), but this increase was not significant ($t = 1.52$; $p =$
380 $.152$). In the sham experiment, the 'time' x 'side' interaction was not significant ($F(1,13) =$
381 1.09 ; $p = .315$).

382 HD-tDCS exerted a significant effect on the latency of the N20 wave. On average, the latency
383 of the N20 wave elicited by stimulation of the contralateral hand was significantly increased
384 after real HD-tDCS but not after sham HD-tDCS (Figure 2). The mixed-model ANOVA showed
385 a significant three-way interaction between the factors 'group', 'time' and 'side' ($F(1,26) =$
386 6.93 ; $p = .014$; Table 1). In the HD-tDCS experiment, the within-subject ANOVA showed a
387 significant 'time' x 'side' interaction ($F(1,13) = 9.24$; $p = .009$), and the post-hoc comparisons
388 confirmed that, after HD-tDCS, the latency of the N20 elicited by stimulation of the
389 contralateral hand was significantly increased ($+0.3 \pm 0.4 \text{ ms}$; $t = 2.51$; $p = .026$), whereas the
390 latency of the N20 elicited by stimulation of the ipsilateral hand was unchanged ($+0.0 \pm 0.4$
391 ms ; $t = .000$; $p = 1.0$). In the sham experiment, the within-subject ANOVA showed no
392 significant 'time' x 'side' interaction ($F(1,13) = 1.43$; $p = .253$; Table 3).

393 **3.3. HFOs elicited by electrical stimulation of the median nerve**

394 In all conditions of both experiments, transcutaneous electrical stimulation of the median
395 nerve elicited a significant burst of HFOs, centered around the latency of the N20 wave.

396 On average, the magnitude of the early subcomponent of HFOs was not changed after real
397 HD-tDCS and after sham HD-tDCS (Fig. 3C). The mixed-model ANOVA showed no main effect
398 of 'time' and no interaction between the factor 'time' and the factors 'group' or 'side'.

399 In contrast, the magnitude of the late subcomponent of HFOs was, on average, increased
400 after HD-tDCS but not after sham HD-tDCS. This was confirmed by the results of the mixed-
401 model ANOVA, which showed a significant interaction between the factors 'time' and
402 'group' ($F(1,26) = 7.03$; $p = .013$; Table 1). In the HD-tDCS group, although the increase in
403 HFOs magnitude was, on average, more pronounced for stimuli delivered to the
404 contralateral hand as compared to the ipsilateral hand, the within-subject ANOVA showed a
405 main effect of 'time' ($F(1,13) = 6.45$; $p = .025$), but no significant 'time' x 'side' interaction
406 ($F(1,13) = 3.82$; $p = .072$; Table 2). In the sham group, the within-subject ANOVA showed no
407 significant changes in HFOs magnitude (Table 3).

408 **3.4. ERPs elicited by non-nociceptive vibrotactile stimulation of the hand dorsum**

409 Non-nociceptive vibrotactile stimuli delivered to the index fingertip elicited a consistent
410 negative-positive potential (N120, P250) maximal at the scalp vertex in each participant and
411 condition (Fig. 2).

412 After real HD-tDCS, the magnitude of the N120 wave was, on average, reduced after
413 stimulation of the hand contralateral to the sensorimotor cortex onto which HD-tDCS was
414 applied, but not after stimulation of the ipsilateral hand. After sham HD-tDCS, the
415 magnitude of the N120 wave was virtually unchanged. This differential effect of real HD-
416 tDCS on the magnitude of the N120 waves elicited by vibrotactile stimulation of the
417 contralateral and ipsilateral hands was confirmed by the results of the mixed-model ANOVA
418 which revealed a significant three-way interaction between the factors 'group', 'time' and

419 'side' ($F(1,26) = 7.35$; $p = .012$). In the HD-tDCS group, the within-subject ANOVA showed a
420 significant 'time' x 'side' interaction ($F(1,13) = 11.03$; $p = .006$), and post-hoc comparison
421 showed that the magnitude of the N120 elicited by stimulation of the contralateral hand
422 was significantly reduced after HD-tDCS ($-3.1 \pm 3.3 \mu\text{V}$; $t = 3.46$; $p = .004$), whereas the
423 magnitude of the N120 elicited by stimulation of the ipsilateral hand was not ($-0.1 \pm 3.5 \mu\text{V}$;
424 $t = .113$; $p = .912$). In the sham group, the within-subject ANOVA showed no significant
425 changes in N120 magnitude (Table 3).

426 Contrasting with the selective effect of real HD-tDCS on the magnitude of the N120 elicited
427 by stimulation of the contralateral hand, the magnitude of the later P250 was, on average,
428 slightly reduced at both hands, both after real HD-tDCS and sham HD-tDCS. This was
429 corroborated by the results of the mixed-model ANOVA, which showed a main effect of
430 'time' ($F(1,26) = 4.76$; $p = .038$), and no interaction between the factor 'time' and the factors
431 'group' or 'side' (Table 1; Fig. 5).

432 The latency of the N120 and P250 were not significantly affected after real or sham HD-tDCS
433 (Fig. 5).

434 **3.5. ERPs elicited by nociceptive laser stimulation**

435 Nociceptive laser stimuli delivered to the hand dorsum elicited a consistent negative-
436 positive complex maximal at the scalp vertex (N240-P350) in each participant and each
437 condition. This complex was preceded by an earlier N160 wave, maximal at central-
438 temporal regions contralateral to the stimulated hand (Fig. 2).

439 After real HD-tDCS, the magnitude of the N240 was, on average, markedly reduced both for
440 stimuli delivered to the ipsilateral hand and for stimuli delivered to the contralateral hand.

441 In contrast, the magnitude of the N240 was virtually unchanged after sham HD-tDCS (Fig. 2;

442 Table 4). This symmetric reduction of the N240 in the HD-tDCS group was confirmed by the
443 results of the mixed-model ANOVA, showing a significant interaction between the factors
444 'group' and 'time' ($F(1,26) = 6.06$; $p = .021$). The within-subject ANOVAs confirmed a main
445 effect of 'time' in the HD-tDCS experiment ($F(1,13) = 13.2$; $p = .003$), and the lack of effect of
446 'time' in the sham experiment ($F(1,13) = 1.0$; $p = .336$).

447 Contrasting with this specific but symmetric effect of HD-tDCS on the magnitude of the
448 N240 wave, the magnitudes of the N160 and P350 waves were, on average, reduced both
449 after real HD-tDCS and after sham HD-tDCS, in a symmetric fashion. The mixed-model
450 ANOVAs revealed a main effect of 'time' (N160: $F(1,26) = 8.33$; $p = .008$; P350: $F(1,26) =$
451 21.9 ; $p < .001$) and no interaction between the factor 'time' and the factors 'group' or 'side'
452 (Table 1).

453 The mixed-model ANOVA showed a marginal interaction between the factors 'time' and
454 'side' on the latency of the N240 wave ($F(1,26) = 4.61$; $p = .041$). However, the within-
455 subject ANOVAs showed no significant differences in N240 latencies, both in the HD-tDCS
456 experiment and in the sham experiment (respectively Table 2 and 3). There was no
457 significant effect of real or sham HD-tDCS on the latencies of the N160 and P350 (Fig. 5).

458 **4. DISCUSSION**

459 Our results show that cathodal HD-tDCS applied over the hand area of the primary
460 sensorimotor cortex exerts a different effect on the cortical processing of non-nociceptive
461 and nociceptive somatosensory input in humans. Specifically, cathodal HD-tDCS significantly
462 affected the responses to non-nociceptive stimuli delivered to the hand contralateral to the
463 sensorimotor cortex onto which HD-tDCS was applied, as demonstrated by the reduced
464 magnitude and increased latency of the N20 wave elicited by electrical stimulation of the

465 contralateral median nerve, and the reduced magnitude of the later-latency N120 wave
466 elicited by vibrotactile stimulation of the contralateral hand dorsum. In contrast, cathodal
467 HD-tDCS of the sensorimotor cortex induced a symmetric effect on the responses to
468 nociceptive stimuli. Rather than reducing the responses elicited by stimulation of the
469 contralateral hand, HD-tDCS led to a symmetric reduction of the N240 wave which was, at
470 least in part, due to a true neuromodulatory of HD-tDCS as it was not observed after sham
471 HD-tDCS.

472 **4.1. HD-tDCS of the sensorimotor cortex decreases the responsiveness of S1**

473 After cathodal HD-tDCS, the magnitude of the N20 wave elicited by stimuli delivered to the
474 contralateral hand was significantly reduced as compared to the N20 wave elicited by
475 stimuli delivered to the ipsilateral hand. This finding is consistent with the results of a
476 previous study showing that cathodal tDCS over the sensorimotor cortex results in a
477 reduction of magnitude of the N20 wave (Dieckhöfer et al. 2006). Considering that the N20
478 wave originates from Brodmann area 3b of S1 and that it constitutes the earliest
479 measurable cortical response to non-nociceptive somatosensory input (Allison et al. 1989a;
480 Hari and Forss 1999; Hari et al. 1984; Valeriani et al. 2004; Valeriani et al. 2000; Wood et al.
481 1985), our finding demonstrates that cathodal HD-tDCS delivered over the sensorimotor
482 cortex significantly reduces the responsiveness of S1 to thalamocortical input ascending
483 within the lemniscal pathways.

484 Further supporting the fact that HD-tDCS exerted an inhibitory effect on S1 was the finding
485 that the latency of the N20 wave elicited by stimulation of the contralateral hand was
486 significantly increased after cathodal HD-tDCS. Because it seems unlikely that HD-tDCS
487 exerts an effect on the time required for somatosensory afferent volleys to reach the cortex,

488 a possible explanation for the increased latency of the N20 peak is that, due to the reduced
489 responsiveness of S1 neurons, generation of the postsynaptic cortical activity leading to the
490 N20 wave required accumulating more afferent input over time. This postsynaptic
491 interpretation is also supported by our finding that HD-tDCS did not modulate early-latency
492 HFOs thought to predominantly reflect synchronized action potentials ascending the
493 thalamocortical projections to S1 (Curio et al. 1997; Hashimoto et al. 1996; Ozaki and
494 Hashimoto 2011; Restuccia et al. 2011).

495 Cathodal HD-tDCS tended to exert an opposite, excitatory effect on the responsiveness of
496 the contralateral S1. Indeed, whereas the magnitude of the N20 wave elicited by stimulation
497 of the contralateral hand was significantly decreased after HD-tDCS, the magnitude of the
498 N20 wave elicited by stimulation of the ipsilateral hand tended to increase (Fig. 2). Because
499 the four return anode electrodes were located immediately adjacent to the cathode
500 electrode, this opposite effect of HD-tDCS on the responsiveness of the contralateral S1
501 cannot be explained by an anodal stimulation of the contralateral hemisphere. One
502 possibility could be that it resulted from inter-hemispheric inhibitory interactions between
503 the left and right sensorimotor cortices (Brodie et al. 2014; Mochizuki et al. 2007; Ragert et
504 al. 2011): applying cathodal HD-tDCS on the sensorimotor cortex could lead to a reduced
505 inter-hemispheric inhibitory drive towards the contralateral homotopic sensorimotor
506 cortex.

507 Finally, cathodal HD-tDCS led to a significant increase of the late-latency HFOs immediately
508 following the N20 wave, and this enhancement was more pronounced for the responses
509 elicited by stimulation of the contralateral median nerve (Fig. 3C). Although this constitutes
510 further evidence that HD-tDCS modulated the state of S1, further studies are needed to

511 understand why HD-tDCS reduced the magnitude of the N20 wave but tended to increase
512 the magnitude of late-latency HFOs. Nevertheless, the genuineness of our results is
513 supported by several previous studies showing that various experimental manipulations can
514 lead to dissociated effects on the N20 wave and HFOs (Gobbele et al. 2003; Katayama et al.
515 2010; Ogawa et al. 2004). Although it is generally assumed that cathodal tDCS decreases
516 cortical responsiveness because it hyperpolarizes the stimulated neurons (Datta et al. 2009;
517 Nitsche et al. 2008; Nitsche and Paulus 2000), Rahman et al. (2013) recently suggested that,
518 during tDCS, different cellular elements can become hyperpolarized or depolarized in any
519 given brain region. Such variable effects could be an explanation for the differential effect of
520 HD-tDCS on the magnitude of the N20 wave and that of late-latency HFOs.

521 **4.2. S1 is an obligatory relay for the higher-order cortical processing of tactile input**

522 Cathodal HD-tDCS delivered over the sensorimotor cortex did not only reduce the early-
523 latency responses to tactile stimuli originating from *within* S1. Indeed, cathodal HD-tDCS
524 also affected later brain responses to vibrotactile stimulation of the contralateral hand,
525 specifically, the N120 wave which is thought to predominantly reflect later stages of cortical
526 processing within the left and right operculo-insular cortex and the cingulate cortex (Allison
527 et al. 1992; Allison et al. 1989b; Garcia-Larrea et al. 1995; Hu et al. 2015; Kunde and Treede
528 1993; Mouraux et al. 2011). Because there was no reduction of the N120 wave elicited by
529 vibrotactile stimuli delivered to the ipsilateral hand, and no reduction of the N120 wave
530 after sham HD-tDCS in the sham experiment, this finding suggests that late responses to
531 tactile stimuli originating from outside S1 are dependent on the state of S1. In other words,
532 this finding provides support for a serial processing of tactile input from the thalamus to S1
533 and from S1 to other brain areas such as the operculo-insular cortex and the cingulate

534 cortex. This interpretation is also supported by the observation of Pons et al. (1992),
535 showing that the responses in S2 to tactile stimuli delivered to the hand of Rhesus monkeys
536 are reduced after lesions of the S1 hand area. However, we cannot exclude that the
537 modulation of the N120 wave observed after HD-tDCS resulted from a neuromodulatory
538 effect of HD-tDCS on other brain regions located close to S1, such as S2 or M1 (see Section
539 4.3).

540 **4.3. Bilateral effect of HD-tDCS on nociceptive processing vs. response habituation**

541 Both the nociceptive ERPs elicited by stimulation of the contralateral hand and the
542 nociceptive ERPs elicited by stimulation of the ipsilateral hand were reduced after cathodal
543 HD-tDCS of the left or right sensorimotor cortex. To examine whether this symmetric
544 reduction of amplitude was due to a neuromodulatory effect of HD-tDCS or to unrelated
545 time-dependent effects such as response habituation (Greffrath et al. 2007) or decreased
546 vigilance (Garcia-Larrea et al. 1997; Legrain et al. 2002; Miltner et al. 1989), we conducted a
547 second experiment in which participants received sham HD-tDCS over the left or right
548 sensorimotor cortex. The reduction of the N240 was present only after real HD-tDCS,
549 indicating that this effect was not merely the consequence of habituation or decreased
550 vigilance. In contrast, the magnitude of the earlier N160 wave and the later P350 wave were
551 similarly reduced after real HD-tDCS and after sham HD-tDCS, suggesting that they could, at
552 least in part, be due to habituation or decreased vigilance.

553 It seems unlikely that the bilateral effect of HD-tDCS on the N240 waves of nociceptive ERPs
554 could be explained by a change in the responsiveness of S1 to ascending nociceptive input,
555 as such a change would be expected to preferentially affect the responses to nociceptive
556 input originating from the contralateral hemibody. Considering the size of the electric field

557 generated by the HD-tDCS montage, it is likely that the effects of HD-tDCS were not
558 restricted to S1, but also extended to nearby areas such as M1 and S2. Furthermore, HD-
559 tDCS can be expected to not only affect the targeted area, but also remote areas having
560 strong connections with the targeted area (Rahman et al. 2013). The bilateral effect of HD-
561 tDCS on the N240 wave of nociceptive ERPs could thus be due, at least in part, to an indirect
562 modulation of other brain areas (Antal and Paulus 2010; Lefaucheur et al. 2006; Mylius et al.
563 2012; Tamura et al. 2004). One possibility could be that the bilateral reduction of the N240
564 resulted from an effect of HD-tDCS on S2 or the highly-connected insular and cingulate
565 cortices, as these areas are thought to be the main sources of the N240, and are known to
566 respond to nociceptive stimuli delivered to both the ipsilateral and contralateral hemibody
567 (Chen et al. 1998; Frot and Mauguiere 2003; Garcia-Larrea et al. 2003; Kakigi et al. 1995;
568 Kanda et al. 2000; Tarkka and Treede 1993; Valeriani et al. 1996; Valeriani et al. 2000; Vogel
569 et al. 2003).

570 Garcia-Larrea et al. showed using PET that direct electrical epidural stimulation of M1 (a
571 procedure sometimes used for the treatment of intractable chronic pain) induces a
572 significant increase in cerebral blood flow in the ipsilateral thalamus, the anterior cingulate
573 and orbitofrontal cortex, the insula and the upper brainstem (Garcia-Larrea et al. 1999). This
574 has led some authors to propose that the rTMS or tDCS delivered over the sensorimotor
575 cortex may activate descending inhibitory control mechanisms acting on the spinal
576 transmission of ascending nociceptive inputs (Garcia-Larrea and Peyron 2007). This
577 hypothesis, which is also supported by the results of Onesti et al. (2013) showing that rTMS
578 delivered over the lower limb representation of M1 in patients suffering from diabetic
579 neuropathic pain leads to a reduction of the spinal nociceptive withdrawal reflex (RIII), could

580 also explain our finding that cathodal HD-tDCS leads to a symmetric reduction of the N240
581 waves of laser-evoked potentials.

582 In addition to reducing the magnitude of the N240 of both hands, HD-tDCS also appeared to
583 reduce the intensity of the percept elicited by laser stimulation of both hands, and this
584 decrease was, on average, more pronounced after real HD-tDCS as compared to sham HD-
585 tDCS. This symmetric effect on pain perception contrasts with the results of some previous
586 studies suggesting that tDCS exerts a stronger effect on the responses elicited by
587 nociceptive stimulation of the contralateral hand (Antal et al. 2008; Csifcsak et al. 2009).
588 However, these studies did not compare directly the responses elicited by stimulation of the
589 ipsilateral and contralateral hands. Furthermore, several previous studies have shown that
590 rTMS or tDCS delivered over the sensorimotor cortex induces a bilateral reduction of pain
591 perception in healthy volunteers (Nahmias et al. 2009; Poreisz et al. 2008b; Terney et al.
592 2008).

593 **4.4. S1 is differentially involved in processing non-nociceptive and nociceptive inputs**

594 Regardless of the mechanism explaining the bilateral and symmetric reduction of
595 nociceptive ERPs after HD-tDCS delivered over the sensorimotor cortex, our finding that
596 cathodal HD-tDCS exerts a clearly lateralized effect on the responses to tactile input
597 originating from the contralateral hand, but does not exert any lateralized effect on the
598 responses to nociceptive input, indicates that S1 is not similarly involved in the processing of
599 non-nociceptive and nociceptive inputs. Considering that the early-latency N160 wave of
600 nociceptive ERPs is thought to reflect, at least in part, activity originating from the
601 contralateral S1, one may wonder why HD-tDCS did not induce a lateralized reduction of the
602 N160, similar to the lateralized reduction of the N20 and N120 elicited by non-nociceptive

603 stimulation. This lack of a lateralized effect suggests that HD-tDCS over the sensorimotor
604 cortex does not similarly affect the ability of S1 to respond to nociceptive and non-
605 nociceptive somatosensory inputs. It has been suggested that area 3b of S1 constitutes the
606 primary target of vibrotactile input, whereas nociceptive input predominantly elicits
607 responses in areas 1 and 2 (Bushnell et al. 1999; Valeriani et al. 2004; Vierck et al. 2013;
608 Whitsel et al. 2009). Differences in the orientation of the cortical surface of the different
609 subregions of S1, being more radial or tangential to the scalp surface, could lead to
610 differential effects of HD-tDCS. Modeling studies have shown that, even directly under the
611 stimulating electrode, tDCS predominantly produces currents that are tangential to the
612 scalp surface, and studies on the effects of direct current stimulation of cortical slices have
613 suggested that the after-effects of tDCS mainly result from changes in the synaptic efficacy
614 of pyramidal neurons whose somatodendritic axis is parallel to the current flow (Rahman et
615 al. 2013).

616 **4.5. Study limitations**

617 A first limitation of our study is the lack of behavioral evidence that HD-tDCS over the
618 sensorimotor cortex modulated the perception of vibrotactile stimuli delivered to the
619 contralateral hand. However, this was also the case in previous studies assessing the effect
620 of cathodal tDCS or TBS over S1 (Grundmann et al. 2011; Torta et al. 2013), and could be
621 related to the fact that subjective reports of the intensity of perception elicited by brief
622 variations of constant amplitude are not a sensitive mean to assess tactile discrimination
623 performance (Tame and Holmes 2016). Future studies should examine whether changes in
624 vibrotaction induced by HD-tDCS over S1 can be identified using more sensitive tasks to

625 assess intensity, frequency or spatial discrimination abilities (Morley et al. 2007; Rogalewski
626 et al. 2004).

627 A second limitation of our study is that the mixed-model ANOVA conducted to compare
628 directly the effects of real HD-tDCS vs. sham HD-tDCS on the magnitude of the N20 wave
629 elicited by electrical stimulation of the median nerve revealed a significant interaction
630 between the factors 'time' (before vs. after HD-tDCS) and 'side' (somatosensory stimuli
631 delivered to the ipsilateral vs. contralateral hand), but no interaction with the factor group
632 (real vs. sham HD-tDCS). This suggests that, even though the lateralized reduction in N20
633 magnitude was clearly more pronounced after real HD-tDCS, a lateralized reduction might
634 also have been present after sham HD-tDCS. This raises the question as to whether HD-tDCS
635 delivered during 110 minutes (40 s ramp-up from 0 to 1 mA, 30 s plateau at 1 mA, 40 s
636 ramp-down from 1 to 0 mA), which is commonly used as a sham condition (Nitsche et al.
637 2008; Tanaka et al. 2009), might actually exert a slight neuromodulatory effect.

638 Finally, because nociceptive laser stimuli were delivered to the hand dorsum and non-
639 nociceptive vibrotactile were delivered to the index fingertip, one should consider whether
640 slight differences in the somatotopic representation of the hand dorsum and index fingertip
641 could have explained the differential effects of HD-tDCS on nociceptive and vibrotactile
642 ERPs. Source analysis studies using MEG (Omori et al. 2013) and high-resolution functional
643 MRI studies (Nelson and Chen 2008) indicate that the distance between the S1 response to
644 nociceptive stimuli delivered to the hand dorsum and vibrotactile stimuli delivered to the
645 index fingertip is below 1 cm, i.e. well below the focus of the HD-tDCS montage used in the
646 present study, which is thought to generate an electric field having a grossly approximate
647 radius of 5 cm. More importantly, considering interindividual variations in anatomy and the

648 fact that the position of the electrodes was defined based on standard scalp locations, slight
649 differences in the location of the cortical patches processing hand dorsum vs. fingertip input
650 cannot be expected to result in a differential effect of HD-tDCS that was consistent across
651 individuals.

652 **4.6. Conclusion**

653 We show that cathodal HD-tDCS delivered over the hand area of the sensorimotor cortex
654 clearly affects the responses to tactile input originating from the contralateral hand in a
655 lateralized fashion, whereas it affects the responses to nociceptive input in a symmetric
656 fashion. Taken together, these results demonstrate, in humans, a differential involvement of
657 S1 in vibrotaction and nociception.

658 **Acknowledgments**

659 **Grants**

660 CL and AM are supported by the European Research council (ERC Starting Grant PROBING
661 PAIN grant number 336130).

662 **Disclosures**

663 No conflicts of interest, financial or otherwise, are declared by the author(s).

664

665 **References**

- 666 **Abraira VE, and Ginty DD.** The sensory neurons of touch. *Neuron* 79: 618-639, 2013.
- 667 **Allison T, McCarthy G, and Wood CC.** The relationship between human long-latency
668 somatosensory evoked potentials recorded from the cortical surface and from the scalp.
669 *Electroencephalogr Clin Neurophysiol* 84: 301-314, 1992.
- 670 **Allison T, McCarthy G, Wood CC, Darcey TM, Spencer DD, and Williamson PD.** Human
671 cortical potentials evoked by stimulation of the median nerve. I. Cytoarchitectonic areas
672 generating short-latency activity. *J Neurophysiol* 62: 694-710, 1989a.
- 673 **Allison T, McCarthy G, Wood CC, Williamson PD, and Spencer DD.** Human cortical
674 potentials evoked by stimulation of the median nerve. II. Cytoarchitectonic areas generating
675 long-latency activity. *J Neurophysiol* 62: 711-722, 1989b.
- 676 **Antal A, Brepohl N, Poreisz C, Boros K, Csifcsak G, and Paulus W.** Transcranial direct current
677 stimulation over somatosensory cortex decreases experimentally induced acute pain
678 perception. *Clin J Pain* 24: 56-63, 2008.
- 679 **Antal A, and Paulus W.** Effects of transcranial theta-burst stimulation on acute pain
680 perception. *Restor Neurol Neurosci* 28: 477-484, 2010.
- 681 **Borckardt JJ, Bikson M, Frohman H, Reeves ST, Datta A, Bansal V, Madan A, Barth K, and
682 George MS.** A pilot study of the tolerability and effects of high-definition transcranial direct
683 current stimulation (HD-tDCS) on pain perception. *J Pain* 13: 112-120, 2012.
- 684 **Brodie SM, Villamayor A, Borich MR, and Boyd LA.** Exploring the specific time course of
685 interhemispheric inhibition between the human primary sensory cortices. *J Neurophysiol*
686 112: 1470-1476, 2014.
- 687 **Bromm B, and Treede RD.** Nerve fibre discharges, cerebral potentials and sensations
688 induced by CO₂ laser stimulation. *Hum Neurobiol* 3: 33-40, 1984.
- 689 **Bushnell MC, Duncan GH, Hofbauer RK, Ha B, Chen JI, and Carrier B.** Pain perception: is
690 there a role for primary somatosensory cortex? *Proc Natl Acad Sci U S A* 96: 7705-7709,
691 1999.
- 692 **Chen ANC, Arendt-Nielsen L, and Plaghki L.** Laser-evoked potentials in human pain: I. Use
693 and possible misuse. *Pain Forum* 7: 174-184, 1998.
- 694 **Chen LM, Dillenburger BC, Wang F, Friedman RM, and Avison MJ.** High-resolution
695 functional magnetic resonance imaging mapping of noxious heat and tactile activations
696 along the central sulcus in New World monkeys. *Pain* 152: 522-532, 2011.

- 697 **Chen LM, Dillenburg BC, Wang F, and Tang CH.** Differential fMRI activation to noxious
698 heat and tactile stimuli in parasyllian areas of new world monkeys. *Pain* 153: 158-169, 2012.
- 699 **Coghill RC, Talbot JD, Evans AC, Meyer E, Gjedde A, Bushnell MC, and Duncan GH.**
700 Distributed processing of pain and vibration by the human brain. *J Neurosci* 14: 4095-4108,
701 1994.
- 702 **Cruccu G, Aminoff MJ, Curio G, Guerit JM, Kakigi R, Mauguiere F, Rossini PM, Treede RD,**
703 **and Garcia-Larrea L.** Recommendations for the clinical use of somatosensory-evoked
704 potentials. *Clin Neurophysiol* 119: 1705-1719, 2008.
- 705 **Csifcsak G, Antal A, Hillers F, Levold M, Bachmann CG, Happe S, Nitsche MA, Ellrich J, and**
706 **Paulus W.** Modulatory effects of transcranial direct current stimulation on laser-evoked
707 potentials. *Pain Med* 10: 122-132, 2009.
- 708 **Curio G, Mackert BM, Burghoff M, Neumann J, Nolte G, Scherg M, and Marx P.**
709 Somatotopic source arrangement of 600 Hz oscillatory magnetic fields at the human primary
710 somatosensory hand cortex. *Neurosci Lett* 234: 131-134, 1997.
- 711 **Datta A, Bansal V, Diaz J, Patel J, Reato D, and Bikson M.** Gyri-precise head model of
712 transcranial direct current stimulation: improved spatial focality using a ring electrode
713 versus conventional rectangular pad. *Brain Stimul* 2: 201-207, 207.e201, 2009.
- 714 **Dieckhöfer A, Waberski TD, Nitsche M, Paulus W, Buchner H, and Gobbelé R.** Transcranial
715 direct current stimulation applied over the somatosensory cortex – Differential effect on
716 low and high frequency SEPs. *Clinical Neurophysiology* 117: 2221-2227, 2006.
- 717 **Dum RP, Levinthal DJ, and Strick PL.** The spinothalamic system targets motor and sensory
718 areas in the cerebral cortex of monkeys. *J Neurosci* 29: 14223-14235, 2009.
- 719 **Edwards D, Cortes M, Datta A, Minhas P, Wassermann EM, and Bikson M.** Physiological
720 and modeling evidence for focal transcranial electrical brain stimulation in humans: a basis
721 for high-definition tDCS. *Neuroimage* 74: 266-275, 2013.
- 722 **Frot M, and Mauguiere F.** Dual representation of pain in the operculo-insular cortex in
723 humans. *Brain* 126: 438-450, 2003.
- 724 **Garcia-Larrea L, Frot M, and Valeriani M.** Brain generators of laser-evoked potentials: from
725 dipoles to functional significance. *Neurophysiol Clin* 33: 279-292, 2003.
- 726 **Garcia-Larrea L, Lukaszewicz AC, and Mauguiere F.** Somatosensory responses during
727 selective spatial attention: The N120-to-N140 transition. *Psychophysiology* 32: 526-537,
728 1995.

- 729 **Garcia-Larrea L, and Peyron R.** Motor cortex stimulation for neuropathic pain: From
730 phenomenology to mechanisms. *Neuroimage* 37 Suppl 1: S71-79, 2007.
- 731 **Garcia-Larrea L, Peyron R, Laurent B, and Mauguiere F.** Association and dissociation
732 between laser-evoked potentials and pain perception. *Neuroreport* 8: 3785-3789, 1997.
- 733 **Garcia-Larrea L, Peyron R, Mertens P, Gregoire MC, Lavenne F, Le Bars D, Convers P,**
734 **Mauguiere F, Sindou M, and Laurent B.** Electrical stimulation of motor cortex for pain
735 control: a combined PET-scan and electrophysiological study. *Pain* 83: 259-273, 1999.
- 736 **Gobbele R, Waberski TD, Thyerlei D, Thissen M, Darvas F, Klostermann F, Curio G, and**
737 **Buchner H.** Functional dissociation of a subcortical and cortical component of high-
738 frequency oscillations in human somatosensory evoked potentials by motor interference.
739 *Neurosci Lett* 350: 97-100, 2003.
- 740 **Greffrath W, Baumgartner U, and Treede RD.** Peripheral and central components of
741 habituation of heat pain perception and evoked potentials in humans. *Pain* 132: 301-311,
742 2007.
- 743 **Grundmann L, Rolke R, Nitsche MA, Pavlakovic G, Happe S, Treede RD, Paulus W, and**
744 **Bachmann CG.** Effects of transcranial direct current stimulation of the primary sensory
745 cortex on somatosensory perception. *Brain Stimul* 4: 253-260, 2011.
- 746 **Hamada M, Murase N, Hasan A, Balaratnam M, and Rothwell JC.** The role of interneuron
747 networks in driving human motor cortical plasticity. *Cereb Cortex* 23: 1593-1605, 2013.
- 748 **Hari R, and Forss N.** Magnetoencephalography in the study of human somatosensory
749 cortical processing. *Philos Trans R Soc Lond B Biol Sci* 354: 1145-1154, 1999.
- 750 **Hari R, Reinikainen K, Kaukoranta E, Hamalainen M, Ilmoniemi R, Penttinen A, Salminen J,**
751 **and Teszner D.** Somatosensory evoked cerebral magnetic fields from SI and SII in man.
752 *Electroencephalogr Clin Neurophysiol* 57: 254-263, 1984.
- 753 **Hashimoto I, Mashiko T, and Imada T.** Somatic evoked high-frequency magnetic oscillations
754 reflect activity of inhibitory interneurons in the human somatosensory cortex.
755 *Electroencephalography and Clinical Neurophysiology/Evoked Potentials Section* 100: 189-
756 203, 1996.
- 757 **Head H, and Holmes G.** Sensory disturbances from cerebral lesions. *Brain* 34: 102-254,
758 1911.
- 759 **Hu L, Mouraux A, Hu Y, and Iannetti GD.** A novel approach for enhancing the signal-to-noise
760 ratio and detecting automatically event-related potentials (ERPs) in single trials. *Neuroimage*
761 50: 99-111, 2010.

762 **Hu L, Zhang L, Chen R, Yu H, Li H, and Mouraux A.** The primary somatosensory cortex and
763 the insula contribute differently to the processing of transient and sustained nociceptive
764 and non-nociceptive somatosensory inputs. *Hum Brain Mapp* 2015.

765 **Huang G, and Mouraux A.** MEP Latencies Predict the Neuromodulatory Effect of cTBS
766 Delivered to the Ipsilateral and Contralateral Sensorimotor Cortex. *PLoS One* 10: e0133893,
767 2015.

768 **Hyvarinen A, and Oja E.** Independent component analysis: algorithms and applications.
769 *Neural Netw* 13: 411-430, 2000.

770 **Kakigi R, Koyama S, Hoshiyama M, Kitamura Y, Shimojo M, and Watanabe S.** Pain-related
771 magnetic fields following painful CO2 laser stimulation in man. *Neurosci Lett* 192: 45-48,
772 1995.

773 **Kanda M, Nagamine T, Ikeda A, Ohara S, Kunieda T, Fujiwara N, Yazawa S, Sawamoto N,
774 Matsumoto R, Taki W, and Shibasaki H.** Primary somatosensory cortex is actively involved
775 in pain processing in human. *Brain Res* 853: 282-289, 2000.

776 **Katayama T, Suppa A, and Rothwell JC.** Somatosensory evoked potentials and high
777 frequency oscillations are differently modulated by theta burst stimulation over primary
778 somatosensory cortex in humans. *Clin Neurophysiol* 121: 2097-2103, 2010.

779 **Kenntner-Mabiala R, Andreatta M, Wieser MJ, Muhlberger A, and Pauli P.** Distinct effects
780 of attention and affect on pain perception and somatosensory evoked potentials. *Biol*
781 *Psychol* 78: 114-122, 2008.

782 **Kunde V, and Treede RD.** Topography of middle-latency somatosensory evoked potentials
783 following painful laser stimuli and non-painful electrical stimuli. *Electroencephalogr Clin*
784 *Neurophysiol* 88: 280-289, 1993.

785 **Kuo HI, Bikson M, Datta A, Minhas P, Paulus W, Kuo MF, and Nitsche MA.** Comparing
786 cortical plasticity induced by conventional and high-definition 4 x 1 ring tDCS: a
787 neurophysiological study. *Brain Stimul* 6: 644-648, 2013.

788 **Lefaucheur JP, Drouot X, Menard-Lefaucheur I, Keravel Y, and Nguyen JP.** Motor cortex
789 rTMS restores defective intracortical inhibition in chronic neuropathic pain. *Neurology* 67:
790 1568-1574, 2006.

791 **Legrain V, Guerit JM, Bruyer R, and Plaghki L.** Attentional modulation of the nociceptive
792 processing into the human brain: selective spatial attention, probability of stimulus
793 occurrence, and target detection effects on laser evoked potentials. *Pain* 99: 21-39, 2002.

794 **Mazzola L, Isnard J, Peyron R, and Mauguiere F.** Stimulation of the human cortex and the
795 experience of pain: Wilder Penfield's observations revisited. *Brain* 135: 631-640, 2012.

- 796 **Miltner W, Johnson R, Jr., Braun C, and Larbig W.** Somatosensory event-related potentials
797 to painful and non-painful stimuli: effects of attention. *Pain* 38: 303-312, 1989.
- 798 **Minhas P, Bansal V, Patel J, Ho JS, Diaz J, Datta A, and Bikson M.** Electrodes for high-
799 definition transcutaneous DC stimulation for applications in drug delivery and
800 electrotherapy, including tDCS. *J Neurosci Methods* 190: 188-197, 2010.
- 801 **Mochizuki H, Furubayashi T, Hanajima R, Terao Y, Mizuno Y, Okabe S, and Ugawa Y.**
802 Hemoglobin concentration changes in the contralateral hemisphere during and after theta
803 burst stimulation of the human sensorimotor cortices. *Exp Brain Res* 180: 667-675, 2007.
- 804 **Morley JW, Vickery RM, Stuart M, and Turman AB.** Suppression of vibrotactile
805 discrimination by transcranial magnetic stimulation of primary somatosensory cortex. *Eur J*
806 *Neurosci* 26: 1007-1010, 2007.
- 807 **Mouraux A, Diukova A, Lee MC, Wise RG, and Iannetti GD.** A multisensory investigation of
808 the functional significance of the "pain matrix". *Neuroimage* 54: 2237-2249, 2011.
- 809 **Mouraux A, Guerit JM, and Plaghki L.** Non-phase locked electroencephalogram (EEG)
810 responses to CO2 laser skin stimulations may reflect central interactions between A partial
811 partial differential- and C-fibre afferent volleys. *Clin Neurophysiol* 114: 710-722, 2003.
- 812 **Mylius V, Borckardt JJ, and Lefaucheur JP.** Noninvasive cortical modulation of experimental
813 pain. *Pain* 153: 1350-1363, 2012.
- 814 **Nahmias F, Debes C, de Andrade DC, Mhalla A, and Bouhassira D.** Diffuse analgesic effects
815 of unilateral repetitive transcranial magnetic stimulation (rTMS) in healthy volunteers. *Pain*
816 147: 224-232, 2009.
- 817 **Nelson AJ, and Chen R.** Digit somatotopy within cortical areas of the postcentral gyrus in
818 humans. *Cereb Cortex* 18: 2341-2351, 2008.
- 819 **Nicholls ME, Thomas NA, Loetscher T, and Grimshaw GM.** The Flinders Handedness survey
820 (FLANDERS): a brief measure of skilled hand preference. *Cortex* 49: 2914-2926, 2013.
- 821 **Nitsche MA, Cohen LG, Wassermann EM, Priori A, Lang N, Antal A, Paulus W, Hummel F,**
822 **Boggio PS, Fregni F, and Pascual-Leone A.** Transcranial direct current stimulation: State of
823 the art 2008. *Brain Stimul* 1: 206-223, 2008.
- 824 **Nitsche MA, and Paulus W.** Excitability changes induced in the human motor cortex by
825 weak transcranial direct current stimulation. *J Physiol* 527 Pt 3: 633-639, 2000.

- 826 **Ogawa A, Ukai S, Shinosaki K, Yamamoto M, Kawaguchi S, Ishii R, and Takeda M.** Slow
827 repetitive transcranial magnetic stimulation increases somatosensory high-frequency
828 oscillations in humans. *Neurosci Lett* 358: 193-196, 2004.
- 829 **Omori S, Iose S, Otsuru N, Nishihara M, Kuwabara S, Inui K, and Kakigi R.** Somatotopic
830 representation of pain in the primary somatosensory cortex (S1) in humans. *Clin*
831 *Neurophysiol* 124: 1422-1430, 2013.
- 832 **Onesti E, Gabriele M, Cambieri C, Ceccanti M, Raccach R, Di Stefano G, Biasiotta A, Truini A,**
833 **Zangen A, and Inghilleri M.** H-coil repetitive transcranial magnetic stimulation for pain relief
834 in patients with diabetic neuropathy. *Eur J Pain* 17: 1347-1356, 2013.
- 835 **Ozaki I, and Hashimoto I.** Exploring the physiology and function of high-frequency
836 oscillations (HFOs) from the somatosensory cortex. *Clin Neurophysiol* 122: 1908-1923, 2011.
- 837 **Penfield W.** Some observations on the cerebral cortex of man. *Proc R Soc Lond B Biol Sci*
838 134: 329-347, 1947.
- 839 **Penfield W, and Boldrey E.** Somatic motor and sensory representation in the cerebral cortex
840 of man as studied by electrical stimulation. *Brain* 60: 389-443, 1937.
- 841 **Plaghki L, Delisle D, and Godfraind JM.** Heterotopic nociceptive conditioning stimuli and
842 mental task modulate differently the perception and physiological correlates of short CO₂
843 laser stimuli. *Pain* 57: 181-192, 1994.
- 844 **Ploner M, Freund HJ, and Schnitzler A.** Pain affect without pain sensation in a patient with a
845 postcentral lesion. *Pain* 81: 211-214, 1999.
- 846 **Ploner M, Gross J, Timmermann L, and Schnitzler A.** Cortical representation of first and
847 second pain sensation in humans. *Proc Natl Acad Sci U S A* 99: 12444-12448, 2002.
- 848 **Pons TP, Garraghty PE, and Mishkin M.** Serial and parallel processing of tactual information
849 in somatosensory cortex of rhesus monkeys. *J Neurophysiol* 68: 518-527, 1992.
- 850 **Poreisz C, Antal A, Boros K, Brepohl N, Csifcsak G, and Paulus W.** Attenuation of N2
851 amplitude of laser-evoked potentials by theta burst stimulation of primary somatosensory
852 cortex. *Exp Brain Res* 185: 611-621, 2008a.
- 853 **Poreisz C, Csifcsak G, Antal A, Levold M, Hillers F, and Paulus W.** Theta burst stimulation of
854 the motor cortex reduces laser-evoked pain perception. *Neuroreport* 19: 193-196, 2008b.
- 855 **Ragert P, Nierhaus T, Cohen LG, and Villringer A.** Interhemispheric interactions between
856 the human primary somatosensory cortices. *PLoS One* 6: e16150, 2011.

857 **Rahman A, Reato D, Arlotti M, Gasca F, Datta A, Parra LC, and Bikson M.** Cellular effects of
858 acute direct current stimulation: somatic and synaptic terminal effects. *J Physiol* 591: 2563-
859 2578, 2013.

860 **Restuccia D, Del Piero I, Martucci L, and Zanini S.** High-frequency oscillations after median-
861 nerve stimulation do not undergo habituation: a new insight on their functional meaning?
862 *Clin Neurophysiol* 122: 148-152, 2011.

863 **Restuccia D, Ulivelli M, De Capua A, Bartalini S, and Rossi S.** Modulation of high-frequency
864 (600 Hz) somatosensory-evoked potentials after rTMS of the primary sensory cortex. *Eur J*
865 *Neurosci* 26: 2349-2358, 2007.

866 **Rogalewski A, Breitenstein C, Nitsche MA, Paulus W, and Knecht S.** Transcranial direct
867 current stimulation disrupts tactile perception. *Eur J Neurosci* 20: 313-316, 2004.

868 **Tame L, and Holmes NP.** Involvement of human primary somatosensory cortex in
869 vibrotactile detection depends on task demand. *Neuroimage* 138: 184-196, 2016.

870 **Tamura Y, Okabe S, Ohnishi T, D NS, Arai N, Mochio S, Inoue K, and Ugawa Y.** Effects of 1-
871 Hz repetitive transcranial magnetic stimulation on acute pain induced by capsaicin. *Pain*
872 107: 107-115, 2004.

873 **Tanaka S, Hanakawa T, Honda M, and Watanabe K.** Enhancement of pinch force in the
874 lower leg by anodal transcranial direct current stimulation. *Exp Brain Res* 196: 459-465,
875 2009.

876 **Tarkka IM, and Treede RD.** Equivalent electrical source analysis of pain-related
877 somatosensory evoked potentials elicited by a CO2 laser. *J Clin Neurophysiol* 10: 513-519,
878 1993.

879 **Terney D, Bergmann I, Poreisz C, Chaieb L, Boros K, Nitsche MA, Paulus W, and Antal A.**
880 Pergolide increases the efficacy of cathodal direct current stimulation to reduce the
881 amplitude of laser-evoked potentials in humans. *J Pain Symptom Manage* 36: 79-91, 2008.

882 **Torta DM, Legrain V, Algoet M, Olivier E, Duque J, and Mouraux A.** Theta burst stimulation
883 applied over primary motor and somatosensory cortices produces analgesia unrelated to
884 the changes in nociceptive event-related potentials. *PLoS One* 8: e73263, 2013.

885 **Towell AD, Purves AM, and Boyd SG.** CO2 laser activation of nociceptive and non-
886 nociceptive thermal afferents from hairy and glabrous skin. *Pain* 66: 79-86, 1996.

887 **Treede RD, Kief S, Holzer T, and Bromm B.** Late somatosensory evoked cerebral potentials
888 in response to cutaneous heat stimuli. *Electroencephalogr Clin Neurophysiol* 70: 429-441,
889 1988.

890 **Tuxhorn IE.** Somatosensory auras in focal epilepsy: a clinical, video EEG and MRI study.
891 *Seizure* 14: 262-268, 2005.

892 **Valentini E, Hu L, Chakrabarti B, Hu Y, Aglioti SM, and Iannetti GD.** The primary
893 somatosensory cortex largely contributes to the early part of the cortical response elicited
894 by nociceptive stimuli. *Neuroimage* 59: 1571-1581, 2012.

895 **Valeriani M, Barba C, Le Pera D, Restuccia D, Colicchio G, Tonali P, Gagliardo O, and Treede**
896 **RD.** Different neuronal contribution to N20 somatosensory evoked potential and to CO₂
897 laser evoked potentials: an intracerebral recording study. *Clin Neurophysiol* 115: 211-216,
898 2004.

899 **Valeriani M, Rambaud L, and Mauguiere F.** Scalp topography and dipolar source modelling
900 of potentials evoked by CO₂ laser stimulation of the hand. *Electroencephalogr Clin*
901 *Neurophysiol* 100: 343-353, 1996.

902 **Valeriani M, Restuccia D, Barba C, Le Pera D, Tonali P, and Mauguiere F.** Sources of cortical
903 responses to painful CO₂ laser skin stimulation of the hand and foot in the human brain.
904 *Clin Neurophysiol* 111: 1103-1112, 2000.

905 **Vierck CJ, Whitsel BL, Favorov OV, Brown AW, and Tommerdahl M.** Role of primary
906 somatosensory cortex in the coding of pain. *Pain* 154: 334-344, 2013.

907 **Villamar MF, Volz MS, Bikson M, Datta A, Dasilva AF, and Fregni F.** Technique and
908 considerations in the use of 4x1 ring high-definition transcranial direct current stimulation
909 (HD-tDCS). *J Vis Exp* e50309, 2013.

910 **Vogel H, Port JD, Lenz FA, Solaiyappan M, Krauss G, and Treede RD.** Dipole source analysis
911 of laser-evoked subdural potentials recorded from parasyllian cortex in humans. *J*
912 *Neurophysiol* 89: 3051-3060, 2003.

913 **Whitsel BL, Favorov OV, Li Y, Quibrera M, and Tommerdahl M.** Area 3a neuron response to
914 skin nociceptor afferent drive. *Cereb Cortex* 19: 349-366, 2009.

915 **Wood CC, Cohen D, Cuffin BN, Yarita M, and Allison T.** Electrical sources in human
916 somatosensory cortex: identification by combined magnetic and potential recordings.
917 *Science* 227: 1051-1053, 1985.

918

919

920 **Figures captions**

921 **Figure 1.** In two separate groups, we assessed the effects of 20 minutes of HD-tDCS vs. sham
922 HD-tDCS over the sensorimotor cortex on the perception and ERPs elicited by non-
923 nociceptive and nociceptive stimuli delivered to the ipsilateral and contralateral hands. The
924 two experiments consisted of two EEG recording sessions, immediately before and
925 immediately after 20 minutes of real HD-tDCS (HD-tDCS experiment) or sham HD-tDCS
926 (sham experiment) of the left or right sensorimotor cortex. During each EEG session, ERPs
927 elicited by non-nociceptive and nociceptive stimuli delivered to the ipsilateral and
928 contralateral hands were recorded. Non-nociceptive stimuli were transcutaneous electrical
929 stimuli delivered to the median nerve at the level of the wrist, and vibrotactile stimuli
930 delivered to the index fingertip. Nociceptive heat stimuli were laser pulses delivered to the
931 hand dorsum. The second recording session always began within 5 minutes after the end of
932 HD-tDCS or sham stimulation, and was completed within 25 minutes.

933

934 **Figure 2.** Non-nociceptive and nociceptive somatosensory ERPs recorded before and after
935 real HD-tDCS (HD-tDCS experiment, left part) and sham HD-tDCS (sham experiment, right
936 part) of the left or right sensorimotor cortex (group-level average waveforms). The N120
937 and P250 waves elicited by vibrotactile stimulation and the N240 and P350 waves elicited by
938 laser stimulation of the ipsilateral and contralateral hand are shown at Cz vs. M1M2. The
939 N20 waves elicited by transcutaneous electrical stimulation of the median nerve are shown
940 at the contralateral parietal electrode (Pc : P3 or P4) vs. Fz. The N160 wave elicited by laser
941 stimulation is shown at the contralateral central electrode (Cc : C3 or C4) vs. Fz. The head
942 plots show the scalp topographies of the different components of non-nociceptive and

943 nociceptive ERPs recorded before (blue frames) and after (red frames) HD-tDCS or sham
944 stimulation. Note the marked reduction of the N120 wave elicited by tactile stimulation of
945 the contralateral hand in the HD-tDCS experiment, the reduction of amplitude and increase
946 of latency of the N20 wave elicited by electrical stimulation of the contralateral median
947 nerve, and the absence of such changes in the sham experiment. Also note the symmetric
948 reduction of the N240 wave in the HD-tDCS experiment, and the lack of such a reduction in
949 the sham experiment.

950

951 **Figure 3. A.** High frequency oscillations (HFOs) elicited by non-nociceptive electrical
952 stimulation of the median nerve can be separated into an early component (red: -5 to 0 ms
953 relative to the latency of the N20 wave) and a late component (blue: 0 to +8 ms relative to
954 the latency of the N20 wave). The dashed line represents the EEG signal band-pass filtered
955 using a 400-1000 Hz Butterworth zero phase filter, the solid line represents its Hilbert
956 transform (average waveform from one recording performed in one subject while
957 stimulating the right hand; contralateral central-parietal electrode CP5 vs. Fz). An estimate
958 of the magnitude of early and late HFOs components was computed by calculating the area
959 under the curve of the Hilbert transform, from -5 to 0 ms (early subcomponent) and from 0
960 to +8 ms (late subcomponent). **B.** Scalp topography of the maximum peak amplitude of
961 HFOs averaged across all participants and all conditions. The amplitude of HFOs was
962 maximal at the contralateral central-parietal electrode (CP5 or CP6 vs. Fz). **C.** Magnitudes of
963 the early and late components of HFOs in the HD-tDCS experiment and the sham
964 experiment. The scatter plots represent for each subject the change in amplitude of the
965 responses elicited by stimulation of the contralateral and ipsilateral hands, after vs. before

966 treatment. The box plots show the group-level average \pm SD. Note, in the HD-tDCS
967 experiment as compared to the sham experiment, the increase in magnitude of late-latency
968 HFOs most evident when stimulating the contralateral hand.

969

970 **Figure 4.** Effect of real HD-tDCS (HD-tDCS experiment) and sham HD-tDCS (sham
971 experiment) on the intensity of the perception elicited by non-nociceptive vibrotactile and
972 nociceptive laser stimuli delivered to the contralateral and ipsilateral hand. The scatter plots
973 represent for each subject the average percentage change in percept before vs. after HD-
974 tDCS or sham stimulation. The box plots show the group-level average \pm SD. Note, the
975 bilateral reduction of the perception elicited by nociceptive laser stimulation, which is most
976 pronounced after real HD-tDCS.

977

978 **Figure 5.** Single-subject and group-level average change in the magnitude of non-
979 nociceptive (N20, N120, P250) and nociceptive (N160, N240, P350) ERPs before vs. after real
980 HD-tDCS (HD-tDCS experiment) and sham HD-tDCS (sham experiment). The black connected
981 lines show the single-subject differences in amplitude (after – before HD-tDCS or sham
982 stimulation) of the responses elicited by stimulation of the ipsilateral and contralateral
983 hands. The box plots show the group-level average \pm SD. Note, in the HD-tDCS experiment,
984 the asymmetric reduction of the N20 and N120 waves elicited by non-nociceptive
985 stimulation of the contralateral hand and the symmetric reduction of the N160 and N240
986 waves elicited by nociceptive stimulation of the contralateral and ipsilateral hands.

987

	Non-nociceptive stimulation							
	time x side x group		time x group		time x side		time	
	F value	p	F value	p	F value	p	F value	p
Intensity of perception	0.15	0.701	0.48	0.495	5.32	0.029*	0.01	0.908
N20 amplitude	2.07	0.163	0.03	0.858	8.42	0.007*	0.00	0.989
N20 latency	6.93	0.014*	1.89	0.181	0.37	0.549	0.68	0.417
N120 amplitude	7.35	0.012*	0.65	0.429	0.08	0.785	3.11	0.09
P250 amplitude	0.57	0.457	0.01	0.921	0.36	0.556	4.76	0.038*
HFOs late subcomponent	0.92	0.347	7.03	0.013*	3.29	0.081	1.36	0.254

	Nociceptive stimulation							
	time x side x group		time x group		time x side		time	
	F value	p	F value	p	F value	p	F value	p
Intensity of perception	0.14	0.716	1.71	0.203	2.97	0.097	11.4	0.002*
N160 amplitude	0.08	0.787	1.27	0.269	0.40	0.531	8.33	0.008*
N240 amplitude	0.47	0.501	6.06	0.021*	0.36	0.556	12.78	0.001*
N240 latency	0.03	0.874	2.12	0.157	4.61	0.041*	0.24	0.625
P350 amplitude	3.46	0.074	0.28	0.602	2.26	0.145	21.91	0.000*

989

990 **Table 1.** Mixed-model ANOVAs with the between-factor 'group' (HD-tDCS experiment vs.
991 sham experiment) and the within-subject factors 'time' (before vs. after HD-tDCS) and 'side'
992 (stimulation of the ipsilateral vs. contralateral hand) * $p < .050$. A three-way 'time' x 'side' x
993 'group' interaction indicates a differential effect of HD-tDCS vs. sham stimulation on the
994 responses to stimuli delivered to the ipsilateral vs. contralateral hand. A two-way 'time' x
995 'group' interaction indicates a bilateral effect of HD-tDCS vs. sham stimulation on the
996 responses to stimuli delivered to both hands; whereas a two-way 'time' x 'side' interaction
997 indicates an asymmetric effect on the responses to stimuli delivered to the ipsilateral vs
998 contralateral hands both after real HD-tDCS and after sham HD-tDCS. Finally, a main effect
999 of 'time' indicates a bilateral change in the responses in both experiments.

1000

	HD-tDCS experiment			
	main effect of 'time'		interaction 'time' x 'side'	
	F value	p	F value	p
Non-nociceptive stimulation				
Intensity of perception	0.40	0.536	2.14	0.167
N20 amplitude	0.01	0.907	9.27	0.009*
N20 latency	2.09	0.172	9.24	0.009*
N120 amplitude	4.05	0.065	11.03	0.006*
P250 amplitude	2.02	0.179	0.62	0.445
HFOs late subcomponent	6.45	0.025*	3.82	0.072
Nociceptive stimulation				
Intensity of perception	9.4	0.009*	0.89	0.362
N160 amplitude	4.88	0.046*	0.05	0.833
N240 amplitude	13.20	0.003*	0.60	0.453
N240 latency	1.59	0.229	2.53	0.136
P350 amplitude	10.82	0.006*	0.08	0.777

1013

1014 **Table 2.** Repeated-measures ANOVAs for the HD-tDCS experiment with the factors 'time'
 1015 (before vs. after HD-tDCS) and 'side' (stimulation of the ipsilateral vs. contralateral hand). *
 1016 p <.050.

1017

	sham experiment			
	main effect of 'time'		interaction 'time' x 'side'	
	F value	p	F value	p
Non-nociceptive stimulation				
Intensity of perception	0.14	0.714	3.19	0.098
N20 amplitude	0.02	0.894	1.09	0.315
N20 latency	0.18	0.679	1.43	0.253
N120 amplitude	0.39	0.545	0.74	0.406
P250 amplitude	2.81	0.118	0.02	0.880
HFOs late subcomponent	1.27	0.280	0.37	0.555
Nociceptive stimulation				
Intensity of perception	2.57	0.133	2.24	0.158
N160 amplitude	4.42	0.056	0.70	0.418
N240 amplitude	1.00	0.336	0.01	0.941
N240 latency	0.57	0.462	2.09	0.172
P350 amplitude	11.56	0.005*	4.55	0.052

1018

1019

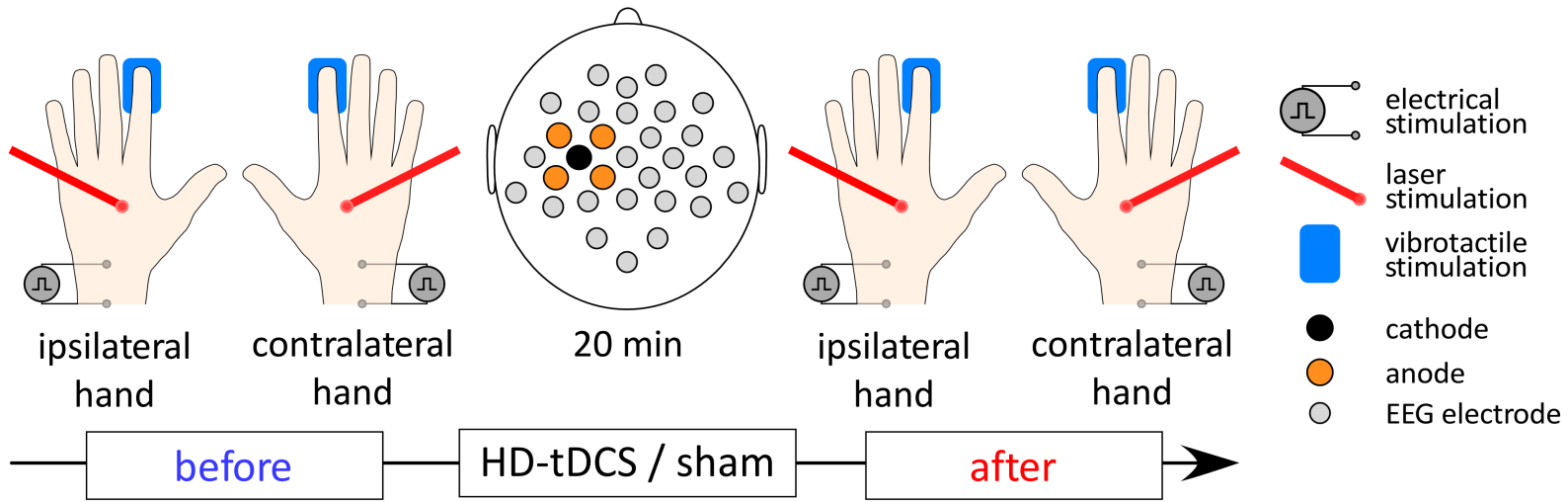
1020 **Table 3.** Repeated-measures ANOVAs for the sham experiment with the factors 'time'
 1021 (before vs. after sham HD-tDCS) and 'side' (stimulation of the ipsilateral vs. contralateral
 1022 hand). * p <.050.

1023

		HD-tDCS experiment				sham experiment			
		contralateral hand		ipsilateral hand		contralateral hand		ipsilateral hand	
		before	after	before	after	before	after	before	after
Non-nociceptive stimulation									
N20	amplitude (μ V)	-2.47 \pm 1.76	-2.15 \pm 1.52	-2.30 \pm 1.42	-2.58 \pm 1.12	-2.14 \pm 0.95	-2.06 \pm 1.13	-2.36 \pm 0.92	-2.48 \pm 1.26
	latency (ms)	19.3 \pm 1.5	19.6 \pm 1.3	19.5 \pm 1.3	19.5 \pm 1.0	19.2 \pm 0.5	19.1 \pm 0.6	19.1 \pm 0.7	19.2 \pm 0.7
N120	amplitude (μ V)	-9.92 \pm 4.94	-6.85 \pm 4.51	-8.70 \pm 5.12	-8.60 \pm 3.62	-6.17 \pm 4.48	-6.08 \pm 4.64	-5.98 \pm 3.89	-4.90 \pm 5.35
	latency (ms)	130 \pm 7	131 \pm 9	130 \pm 11	135 \pm 9	124 \pm 15	126 \pm 12	125 \pm 14	127 \pm 14
P250	amplitude (μ V)	16.7 \pm 6.56	15.2 \pm 5.23	16.2 \pm 5.55	15.5 \pm 5.14	17.1 \pm 5.78	15.9 \pm 5.68	17.5 \pm 5.26	16.3 \pm 5.26
	latency (ms)	233 \pm 44	248 \pm 45	247 \pm 43	247 \pm 40	258 \pm 56	265 \pm 49	244 \pm 47	276 \pm 43
HFOs	early component (μ V.ms)	0.130 \pm 0.064	0.137 \pm 0.062	0.100 \pm 0.040	0.109 \pm 0.039	0.121 \pm 0.045	0.117 \pm 0.047	0.118 \pm 0.049	0.124 \pm 0.023
	late component (μ V.ms)	0.106 \pm 0.055	0.135 \pm 0.068	0.115 \pm 0.064	0.118 \pm 0.044	0.092 \pm 0.027	0.090 \pm 0.021	0.109 \pm 0.032	0.099 \pm 0.033
Intensity of perception (NRS)		2.8 \pm 1.7	2.6 \pm 1.6	2.8 \pm 1.6	2.6 \pm 1.5	2.6 \pm 1.1	2.8 \pm 1.3	2.8 \pm 1.3	2.8 \pm 1.2
Nociceptive stimulation									
N160	amplitude (μ V)	-9.29 \pm 6.27	-6.73 \pm 4.42	-9.46 \pm 8.83	-6.67 \pm 5.42	-5.96 \pm 4.34	-5.07 \pm 3.47	-6.68 \pm 5.75	-5.23 \pm 5.78
	latency (ms)	175 \pm 20	178 \pm 16	176 \pm 20	182 \pm 21	179 \pm 28	188 \pm 25	182 \pm 29	184 \pm 25
N240	amplitude (μ V)	-19.7 \pm 12.7	-14.0 \pm 10.1	-20.6 \pm 15.6	-13.3 \pm 10.3	-13.2 \pm 10.3	-12.0 \pm 9.67	-12.5 \pm 8.60	-11.3 \pm 9.81
	latency (ms)	219 \pm 21	219 \pm 19	208 \pm 24	222 \pm 26	224 \pm 21	215 \pm 28	223 \pm 21	226 \pm 27
P350	amplitude (μ V)	21.7 \pm 11.02	16.0 \pm 11.92	21.3 \pm 11.66	15.9 \pm 14.00	15.6 \pm 9.67	13.0 \pm 7.04	17.8 \pm 8.65	11.6 \pm 6.99
	latency (ms)	326 \pm 31	326 \pm 34	325 \pm 33	339 \pm 41	344 \pm 44	352 \pm 53	341 \pm 43	337 \pm 48
Intensity of perception (NRS)		4.4 \pm 1.8	3.9 \pm 2.1	4.5 \pm 1.7	3.8 \pm 2.2	3.8 \pm 1.3	3.7 \pm 1.4	3.9 \pm 1.1	3.6 \pm 1.3

1024

1025 **Table 4.** Group-level average (\pm SD) ERP magnitude (μ V), ERP latency (ms), HFO amplitude (μ V.ms) and intensity of perception (numerical rating
1026 scale extending between 0 and 10) obtained before and after real or sham HD-tDCS, following stimulation of the ipsilateral or contralateral
1027 hand.



non-nociceptive ERPs

HD-tDCS experiment

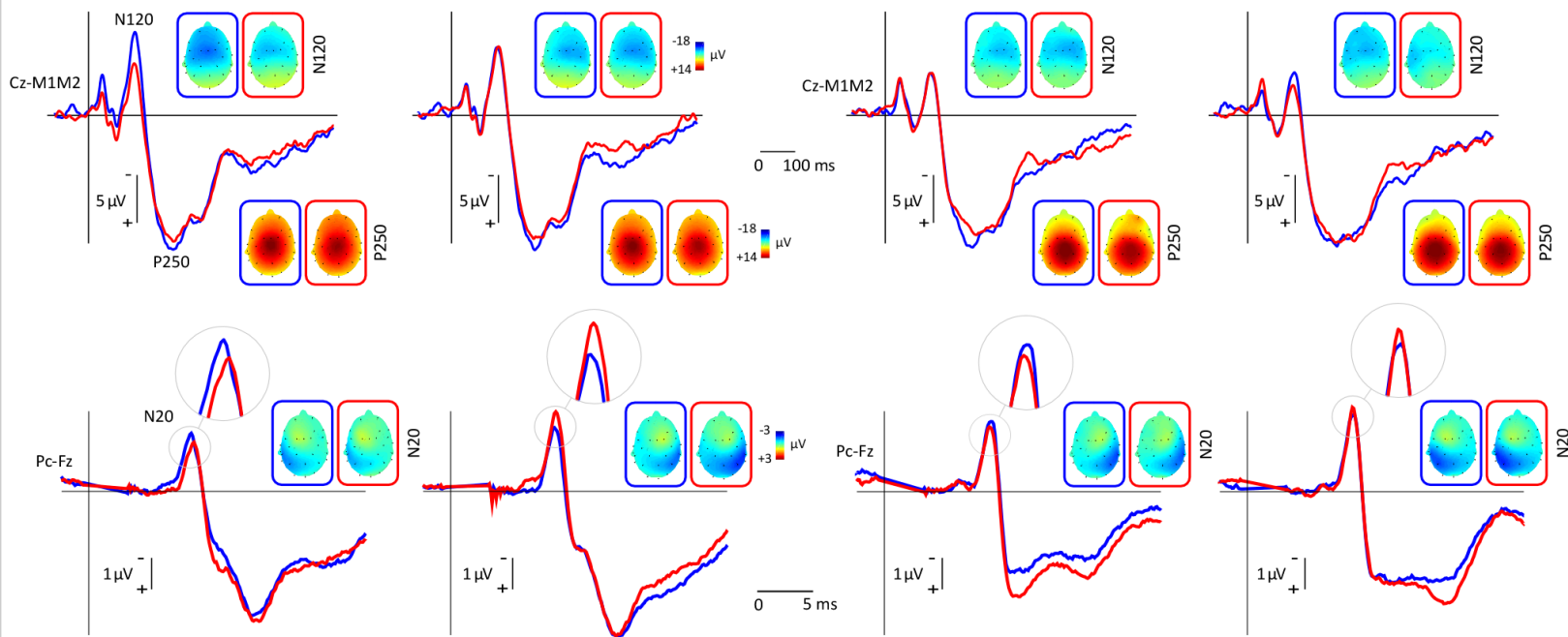
sham experiment

contralateral hand

ipsilateral hand

contralateral hand

ipsilateral hand



nociceptive ERPs

HD-tDCS experiment

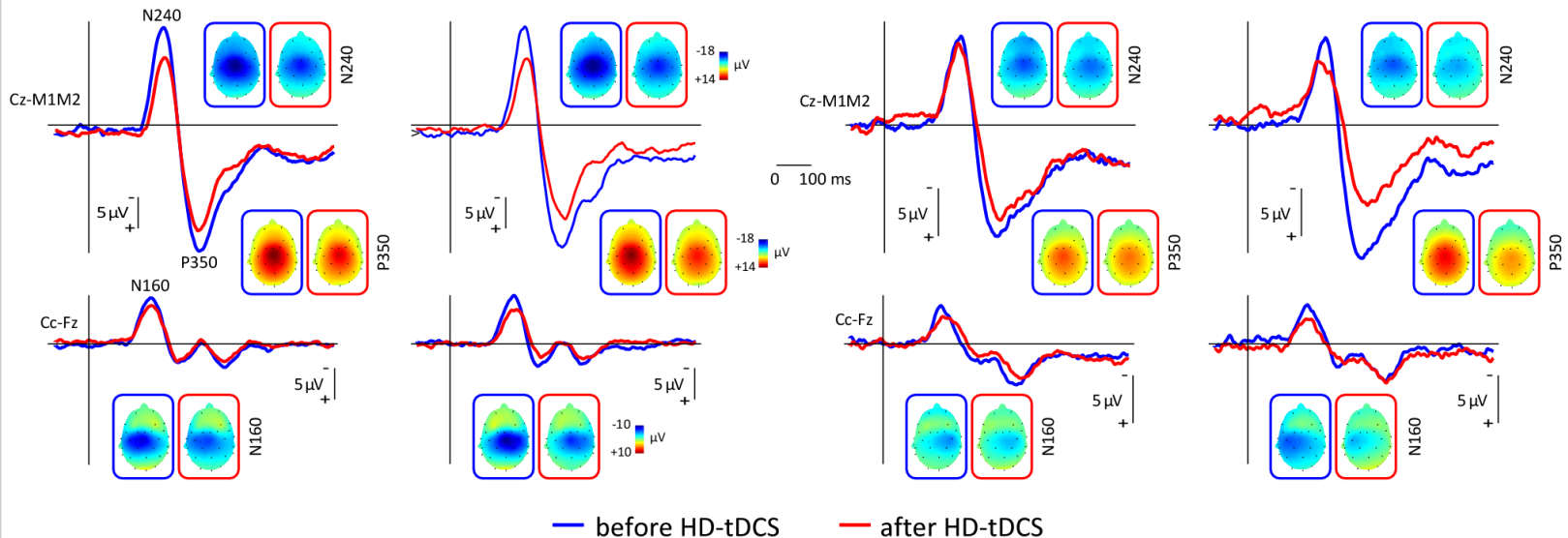
sham experiment

contralateral hand

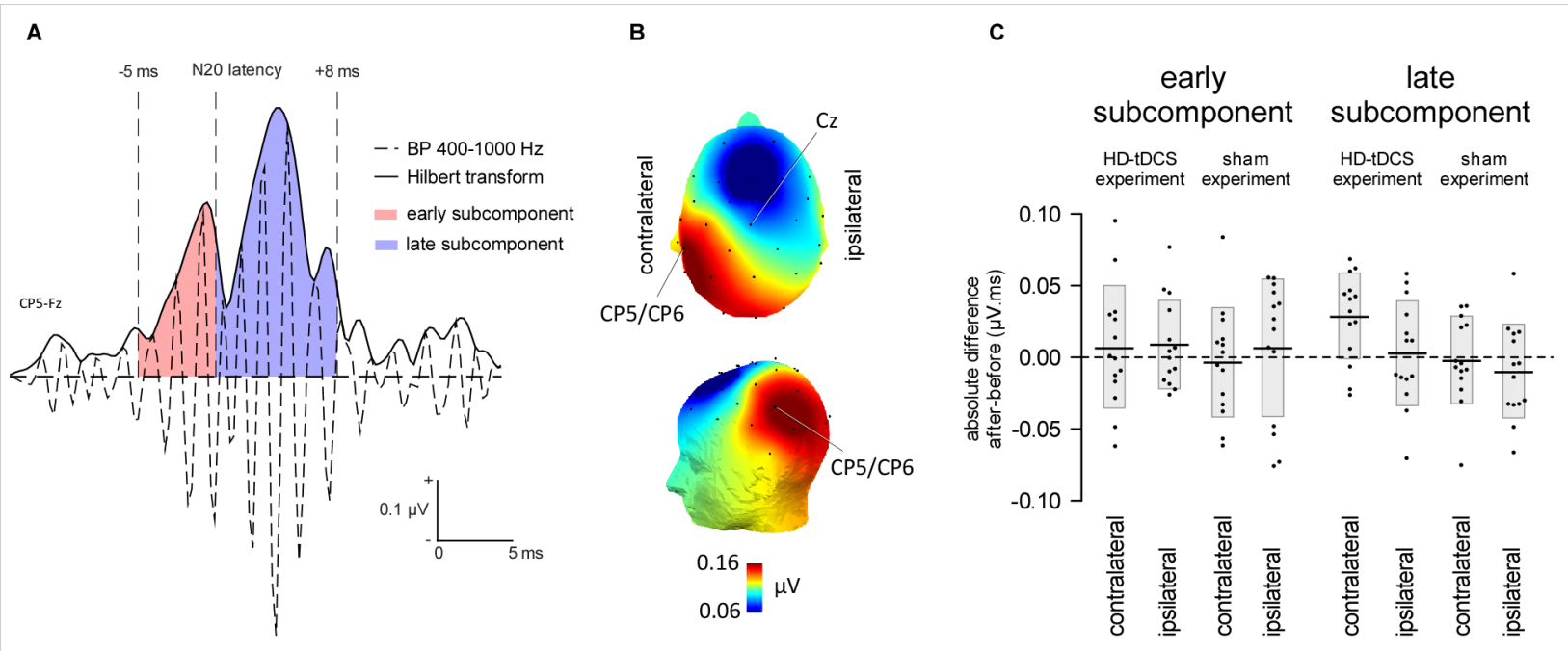
ipsilateral hand

contralateral hand

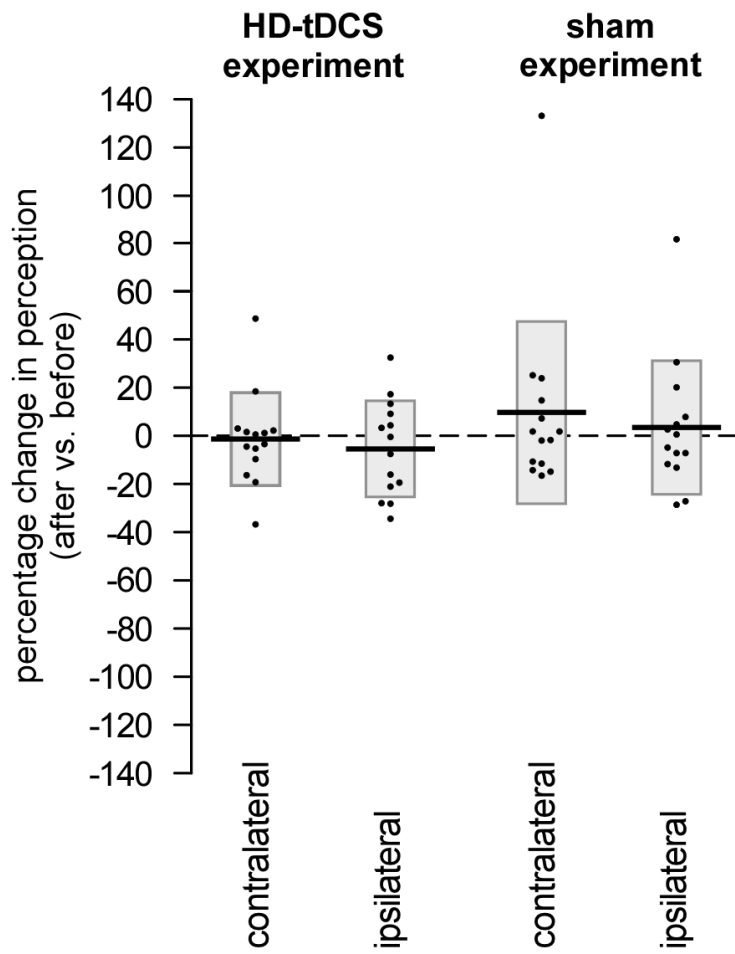
ipsilateral hand



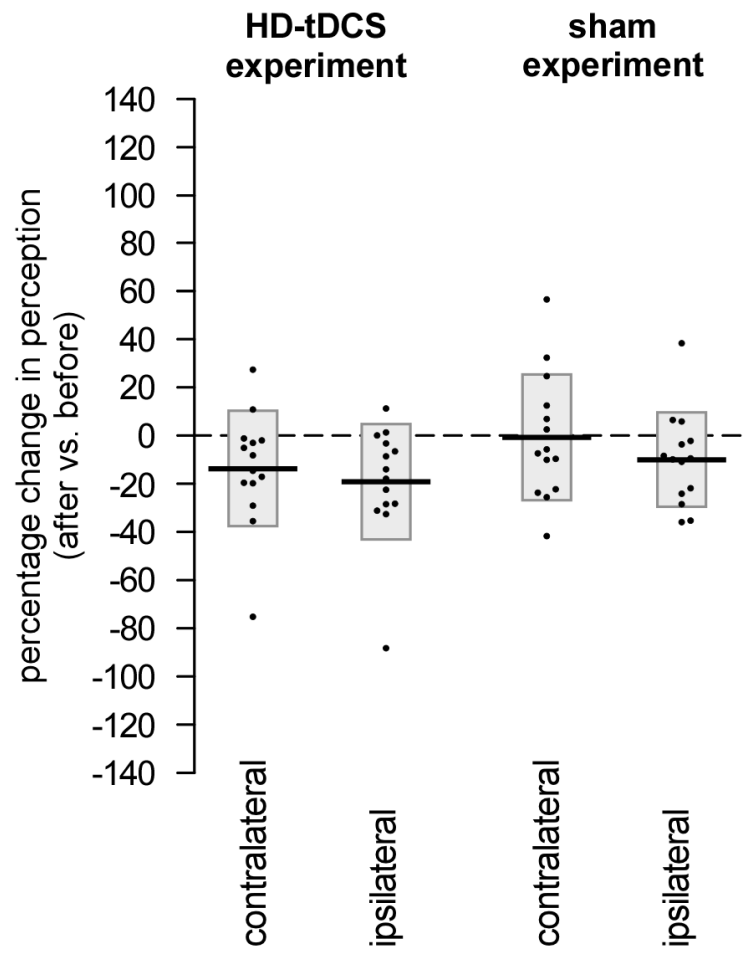
— before HD-tDCS — after HD-tDCS



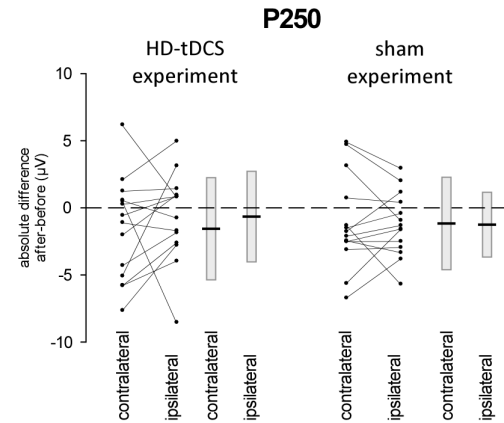
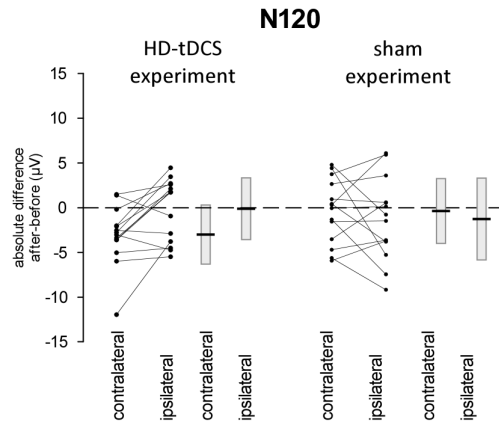
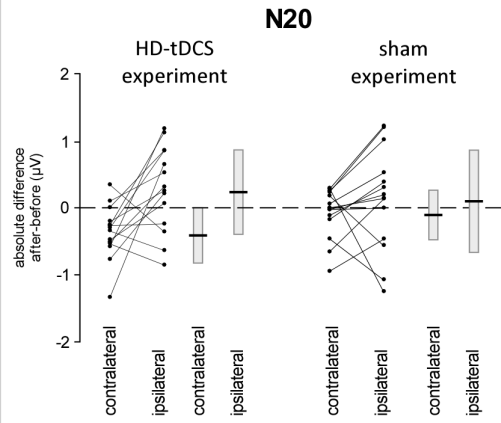
non-nociceptive stimulation



nociceptive stimulation



non-nociceptive ERPs



nociceptive ERPs

